BMJ Open

Multiparametric MRI Detects Subclinical Tissue Injury in Asymptomatic Spinal Cord Compression

Journal:	*BMJ Open*
Manuscript ID	bmjopen-2017-019809
Article Type:	Research
Date Submitted by the Author:	27-Sep-2017
Complete List of Authors:	Martin, Allan; University of Toronto, Department of Surgery De Leener, Benjamin; École Polytechnique de Montréal Cohen-Adad, Julien ; Polytechnique Montreal Cadotte, David; University of Calgary, Department of Neurosurgery Nouri, Aria; University of Toronto, Department of Surgery Wilson, Jefferson; University of Toronto, Department of Surgery Tetreault, Lindsay; University of Toronto, Department of Surgery; University College Cork, Department of Medicine Crawley, Adrian; University of Toronto, Department of Medical Imaging Mikulis, David; University of Toronto, Department of Medical Imaging Ginsberg, Howard; University of Toronto, Department of Medical Imaging Fehlings, Michael
Primary Subject Heading:	Neurology
Secondary Subject Heading:	Radiology and imaging, Diagnostics
Keywords:	quantitative MRI, diffusion tensor imaging, magnetization transfer, myelopathy, spinal cord injury, preclinical

Multiparametric MRI Detects Subclinical Tissue Injury in Asymptomatic Spinal Cord Compression

Allan R. Martin, MD, PhD[1],
Benjamin De Leener, MSc[2], Julien Cohen-Adad, PhD[2],
David W. Cadotte, MD, PhD[3], Aria Nouri, MD, MSc[1], Jefferson R. Wilson, MD, PhD[1],
Lindsay Tetreault, PhD[1,4], Adrian Crawley, PhD[5], David J. Mikulis, MD, PhD[5],
Howard Ginsberg, MD, PhD[5], Michael G. Fehlings, MD, PhD[5]

[1]Division of Neurosurgery, Department of Surgery, University of Toronto, Toronto, ON, Canada,
[2]Electrical Engineering, École Polytechnique de Montréal, Montréal, QC, Canada,
[3]Department of Neurosurgery, University of Calgary, Calgary, AB, Canada,
[4]Department of Medicine, University College Cork, Cork, Ireland,
[5]Department of Medical Imaging, University of Toronto, Toronto, ON, Canada

[#]Address correspondence and reprint requests to Michael G Fehlings, MD, PhD, FRCSC, FACS. Division of Neurosurgery, Toronto Western Hospital, 399 Bathurst St. Suite 4WW-449, Toronto, Ontario, M5T 2S8, Canada; Fax: 416-603-5298, Tel: 416-603-5072, E-mail: michael.fehlings@uhn.on.ca

Data Statement: Technical appendix, statistical code, and dataset available will be uploaded to the Dryad repository prior to publication.

Running title: qMRI detects subclinical spinal cord tissue injury

Word Count: 3784

Abstract

Objectives: Degenerative cervical myelopathy (DCM) involves extrinsic spinal cord (SC) compression causing tissue injury and neurological dysfunction. Asymptomatic SC compression (ASCC) is more common but its significance is poorly defined. This study investigates if: 1) ASCC can be diagnosed using SC shape analysis; 2) multi-parametric quantitative MRI (qMRI) can detect similar SC tissue injury as previously observed in DCM.

Design: Prospective longitudinal cohort study.

Setting: Single centre, tertiary care and research institution.

Participants: 40 neurologically intact subjects (19 female, 21 male) recruited by convenience sampling.

Interventions: Subjects underwent 3T MRI to calculate cross-sectional area (CSA), diffusion fractional anisotropy (FA), magnetization transfer ratio (MTR), and T2*-weighted imaging white to grey matter signal intensity ratio (T2*WI WM/GM). qMRI data were extracted from rostral (C1-3), caudal (C6-7), and maximally compressed levels (MCL). Diagnosis of SC compression was performed with automated shape analysis of flattening, indentation, and torsion. Ten qMRI measures were analyzed individually and as a composite (averaged z scores). Subjects were followed longitudinally for 1-2 years for symptoms and signs of myelopathy development.

Outcome Measures: SC CSA, FA, MTR, and T2*WI WM/GM.

Results: ASCC was present in 20/40 subjects. Shape analysis provided diagnostic accuracy > 97%. Five qMRI metrics demonstrated evidence of tissue injury in ASCC ($p<0.05$), while composite score showed stronger differences ($p=0.002$). At follow-up (median 21 months), two ASCC subjects developed DCM.

Conclusions: Myelopathy occurs prior to the onset of neurological symptoms and signs, with SC compression causing subclinical tissue injury. ASCC is a prevalent age-related preclinical state that can be objectively diagnosed with shape analysis. ASCC appears to carry an increased risk of symptomatic myelopathy development, and these subjects should be educated and monitored for symptom development. These findings offer the intriguing possibility of pre-symptomatic diagnosis and treatment of DCM and other spinal pathologies.

Registration: Not applicable.

Strengths and Limitations of this Study

Strengths:

- The development of novel spinal cord shape analysis to objectively define and detect subtle spinal cord compression
- Use of cutting-edge MRI techniques that are suitable for clinical translation to detect pre-symptomatic spinal cord tissue injury
- Multiple measures of tissue injury that cross-validate each other and can be combined as a composite to increase statistical power

Limitations:

- Lack of histopathological correlation data to confirm the presence of tissue injury
- Modest sample size makes it difficult to draw conclusions about the clinical relevance of asymptomatic cord compression because the rate of progression to symptomatic myelopathy is not well defined.

Funding

This research received funding from Rick Hansen Institute, grant number RHI-2014-12, as part of the Riluzole in Spinal Cord Injury Study (RISCIS), which is also supported by AOSpine North America, AOSpine International SCI Knowledge Forum, and the North American Clinial Trials Network (NACTN) of the Christopher and Dana Reeve Foundation. This research also received support from the Dezwirek Foundation, the Sherman Clinical Research Unit, and the Gerald and Tootsie Halbert Chair in Spinal Cord Research. Dr. Martin received post-doctoral fellowship support from Canadian Institutes of Health Research, grant number 201511MFE-359116-246227.

Conflicts of Interest

The authors declare no conflicts of interest for this manuscript.

Keywords: quantitative MRI, diffusion tensor imaging, magnetization transfer, myelopathy, spinal cord injury, preclinical

Introduction

Degenerative cervical myelopathy (DCM) involves age-related degeneration of the discs, ligaments, and vertebrae leading to extrinsic spinal cord (SC) compression and neurological dysfunction.[1] The prevalence of DCM is difficult to estimate, but it has been suggested that it is probably the most common cause of SC dysfunction.[1,2] However, asymptomatic SC compression (ASCC) is far more frequent, with prevalence estimates ranging from 8% to 59%.[3-8] Furthermore, SC compression may be underestimated using supine MRI, which misses dynamic compression that is visible with flexion/extension MRI.[9] ASCC has received little research attention, but one study found that it confers an increased risk of myelopathy development.[10]

Emerging quantitative MRI (qMRI) techniques offer in vivo measurement of SC microstructural features and tissue injury.[11-13] Cross-sectional area (CSA) measures SC compression and atrophy, the diffusion tensor imaging (DTI) metric fractional anisotropy (FA) measures axonal integrity, magnetization transfer ratio (MTR) reflects myelin quantity, and T2*-weighted imaging (T2*WI) white matter to grey matter signal intensity ratio (T2*WI WM/GM) is a novel biomarker that we recently introduced that correlates with demyelination, gliosis, calcium, and iron concentrations.[12,14,15] These measures hold potential for earlier diagnosis of various conditions, but results to date have been modest and insufficient to drive clinical adoption.[11,13]

Our group previously reported a clinically feasible multiparametric qMRI protocol that measures CSA, FA, MTR, and T2*WI WM/GM across the cervical SC.[14,15] In DCM patients, these metrics reveal macro- and microstructural changes at the maximally compressed level (MCL) and in the uncompressed SC above and below; significant clinical correlations and group differences compared with healthy subjects were found at rostral, MCL, and caudal levels for FA and T2*WI WM/GM, while CSA and MTR showed significant results at rostral and MCL levels.[15] In the current study, we test the hypothesis that subjects with ASCC experience tissue injury compared with uncompressed subjects, based on the same ten qMRI measures. We establish an objective definition of SC compression and assess newly developed automated SC shape analysis for diagnostic accuracy. Finally, we investigate the rate of symptomatic myelopathy development at follow-up and associated risk factors.

Methods

Study Design and Subjects

This study involved a secondary analysis of prospectively collected data that has been previously reported,[14,15] and received institutional approval from University Health Network (UHN, Toronto, Ontario, Canada). 42 subjects were recruited between October 2014 and December 2016 by convenience sampling and provided written informed consent. All clinical data collection and physical examinations were performed by a physician member of the UHN Spine Program. Subjects were examined to rule out neurological symptoms (numbness, weakness, fine motor dysfunction, gait/balance difficulties, urinary urgency/incontinence) and signs (hyperreflexia, weakness, sensory deficits, Romberg sign, gait ataxia). Neck pain was not considered a neurological symptom. Subjects were also required to have 18/18 on the modified Japanese Orthopedic Association score. Two

subjects were excluded during screening; one showed gait ataxia and both had sensory deficits, hyperreflexia, and MRI evidence of SC compression consistent with DCM. Follow-up assessments were performed by telephone, including mJOA administration. Subjects that reported any neurological symptoms underwent a complete neurological examination in person.

MRI Acquisitions

Subjects underwent T2-weighted imaging (T2WI), DTI, magetization transfer (MT), and T2*WI at 3T (GE Signa Excite HDxt) covering C1-C7, as previously described.[14] DTI, MT, and T2*WI images were acquired with 13 axial slices from C1 to C7. T2WI was performed with a FIESTA-C sequence with 0.8x0.8x0.8 mm^3 isotropic resolution. DTI used spin-echo single shot echo planar imaging (ssEPI) with 3 acquisitions averaged offline, b = 800 s/mm^2 in 25 directions, 5 images with b=0 s/mm^2, and resolution of 1.25x1.25x5 mm^3. MT used 2D spoiled gradient echo ± MT pre-pulse, with 1x1x5mm^3 voxels. T2*WI acquisition used multi-echo recombined gradient echo (MERGE) with 3 echoes at 5,10,15 ms and resolution 0.6x0.6x4 mm^3. Total imaging time was 30-35 minutes including patient positioning, slice prescription, and 2nd order localized shimming (prior to DTI).

Image Analysis

Images were inspected and excluded from analysis if image quality was poor or artifacts were present. Quantitative imaging data were analyzed using Spinal Cord Toolbox (SCT) v3.0,[16] including SC segmentation, registration to the probabilistic SCT template, and extraction of metrics with partial volume correction, as previously described.[14,15] Segmentations and registered images were reviewed, and if necessary segmentations were manually edited to correct inaccuracies.

Diagnosis of SC compression followed a 3-step process. First, anatomical images (T2WI and T2*WI) were independently examined by 2 raters (ARM, AN) for indentation, flattening, torsion, or circumferential compression from extrinsic tissues (disc, ligament, or bone). Discrepancies were resolved by consensus. Effacement of the cerebrospinal fluid (CSF) was noted but not considered compression. Second, automated shape analysis was performed on each axial section of the T2*WI SC segmentation mask. 2D principle component analysis (PCA) identified the long and short axes, representing transverse and anterior-posterior (AP) directions, respectively (Figure 1). Flattening was measured with compression ratio (CR) = AP/transverse diameter.[17] Indentation was measured using solidity = the percentage of area representing SC within the convex hull that subtends the SC. Torsion was measured with relative rotation, which was calculated as the angle between transverse axis and horizontal, relative to adjacent slices (difference from the average rotation of above and below slices). Circumferential compression was not specifically measured with a shape metric, as it typically coincides with flattening. Receiver operating characteristic (ROC) curves were plotted to determine diagnostic accuracy of shape metrics at each intervertebral level compared with consensus ratings. Third, discrepancies were discussed and diagnoses were revised if necessary. Normative values for shape parameters were calculated in uncompressed subjects. ROC curves were utilized to calculate revised diagnostic accuracy and optimal diagnostic thresholds (using Youden's Index). Analysis of variance (ANOVA) and Levene's test assessed if mean and variance of shape metrics varied among rostro-caudal levels, respectively. Pooled mean, SD, and diagnostic thresholds were calculated if levels showed no differences.

Tissue injury was measured with CSA of the SC, and FA, MTR, and T2*WI WM/GM extracted from WM. Metrics were normalized for rostro-caudal level and averaged across rostral (C1-3), middle (C4-5 in uncompressed subjects or maximally compressed level, MCL, in ASCC subjects), and caudal (C6-7) levels. The MCL for subjects with multilevel compression was determined by consensus ratings after considering automated shape results. For MCL measurements, data from a single level was used for CSA, whereas 3 slices centered at MCL were averaged for FA, MTR, and T2*WI WM/GM. Non-CSA metrics were also extracted from the ventral columns (VCs), lateral columns (LCs), dorsal columns (DCs) and GM averaged across C1-C7 to identify focal injury. Metrics were normalized for age, sex, height, weight, and cervical cord length, similar to our previous approach,[14] based on multiple linear regression with backward stepwise variable selection. However, the presence of SC compression was included to measure independent effects of other variables, and age was retained regardless of significance to mitigate the discrepancy between groups. Ratios of MCL/rostral metrics were also calculated.[18]

Statistical Analysis

Statistical analysis was performed with R v3.3. Numerical data were summarized by mean ± standard deviation (SD). Binary variables were compared using Fisher exact tests, whereas numerical variables used two-tailed Welch's T tests (demographic data) or Wilcoxon tests (normalized qMRI metrics). 95% confidence intervals (CIs) for frequencies were calculated using the Wilson procedure with continuity correction. The z scores of individual qMRI metrics (using negative values for T2*WI WM/GM) were averaged to yield a composite score, following a t distribution with 10 degrees of freedom (t_{10}). A binomial test compared the pattern of differences in ASCC with that in DCM.[15] Logistic regression with backward stepwise elimination was used to develop a model for detecting tissue injury, retaining a maximum of 4 qMRI metrics as independent variables. Age, sex, and baseline qMRI metrics were analyzed for prediction of myelopathy development using Wilcoxon tests, Fisher exact tests, and logistic regression. Significance was set at $p < 0.05$, including individual measurements of $|z| > 1.96$, $|t_{10}| > 2.23$, and $|t_9| > 2.26$.

Results

Subject Characteristics

Subject characteristics are listed in Table 1. Individuals with ASCC were older (54.9 vs. 39.4, p=0.0007) and weighed more (79.8 vs. 71.1, p=0.03) than subjects without cord compression, while other characteristics (sex, height, and neck length) did not differ.

Table 1: Subject Characteristics. Demographics and clinical measures are tabulated for subjects with and without cervical spinal cord compression. ** denotes significant differences ($p < 0.05$) between groups.

Characteristic	Uncompressed Subjects (N=20)	Compressed Subjects (N=20)	P value
Age	39.4 ± 12.8	54.9 ± 13.8	0.0007**
Sex (M:F)	10:10	11:9	1.0
Height (cm)	172.7 ± 9.4	170.5 ± 8.0	0.43
Weight (kg)	71.1 ± 10.4	79.8 ± 13.3	0.03**
Neck Length (mm)	106.3 ± 9.6	107.0 ± 9.4	0.81

Diagnosis of Spinal Cord Compression

Consensus ratings identified 19 subjects with SC compression at 41 levels (flattening: 20 levels, indentation: 30 levels, torsion: 8 levels, circumferential compression: 1 level). Relative to these ratings, automated shape analysis achieved AUC=99.2% for flattening, AUC=97.3% for indentation, and AUC=97.7% for torsion (Table 2). After reviewing shape analysis results, 3 levels were reclassified as flattened (total: 23 levels) and 1 level as indented (total: 31 levels). Remaining discrepancies were mostly at adjacent levels, which showed a transition between normal and abnormal shape. Using revised diagnoses and excluding adjacent levels, diagnostic accuracy of shape analysis improved to 99.8% for flattening, 99.3% for indentation, and 98.4% for torsion. CR differed across rostrocaudal levels, whereas solidity and relative rotation appeared to be invariant, yielding pooled normative values of 96.52 ± 0.56% and 0.3 ± 1.5 degrees, respectively.

Table 2: Shape Metrics. Data for CR, solidity, and relative rotation are displayed for each intervertebral level from C2-C7. Normal data are derived from 20 subjects with no cord compression and reported as mean ± SD. Diagnostic accuracy is reported as AUC relative to consensus ratings (prior to revision incorporating these results). AUC: area under the curve, CR: compression ratio, ROC: receiver operating characteristic function, SD: standard deviation.

Shape Parameter	Statistic	C2-3	C3-4	C4-5	C5-6	C6-7	Pooled Values
CR (%)	Normal Mean ± SD	67.2 ± 6.4	62.6 ± 5.1	59.3 ± 4.5	59.2 ± 4.2	58.7 ± 4.5	-
	Flattened Frequency	0/40	3/40	5/40	9/40	6/40	23/200
	AUC	-	1.00	0.989	1.0	0.977	0.992
	Diagnostic Threshold	-	53.1	52.0	49.9	50.5	-
Solidity (%)	Normal Mean ± SD	96.52 ± 0.47	96.25 ± 0.53	96.74 ± 0.59	96.64 ± 0.46	96.45 ± 0.76	96.52 ± 0.56
	Indented Frequency	0/40	6/40	11/40	9/40	5/40	31/200
	AUC	-	0.979	0.964	0.971	0.978	0.973
	Diagnostic Threshold	-	-	-	-	-	95.5
Relative Rotation (Degrees)	Normal Mean ± SD	0.0 ± 1.3	0.5 ± 1.6	0.5 ± 1.3	0.4 ± 1.4	0.3 ± 1.5	0.3 ± 1.5
	Rotated Frequency	0/40	1/40	0/40	3/40	4/40	8/200
	AUC	-	0.982	-	0.978	0.971	0.977
	Diagnostic Threshold	-	-	-	-	-	3.3

Final diagnostic ratings identified ASCC in 20/40 subjects (50%, 95% CI: 34.1-65.9%). Six additional subjects (15%) without compression had effacement of the CSF. The frequency of ASCC increased with age (Figure 2), including 15/21 (71.4%, 95% CI: 47.7-87.8%) among subjects aged ≥ 50.

Details of SC compression and shape metrics for each of the 20 ASCC subjects are provided in Supplemental Table 1. SC compression was primarily anterior at all compressed levels, related to disc ± osteophyte complexes (DOCs), with an element of posterior compression due to ligamentum flavum (LF) hypertrophy at 9 levels. T2WI hyperintensity was not present in any subject, although 1 had a prominent central canal (1mm diameter, within normal limits).

Variation of MRI Metrics with Age and Other Characteristics

CSA varied with cervical cord length and MTR varied with height at rostral and MCL levels, independent of the effect of cord compression (Supplemental Table 2). None of the metrics varied significantly with age.

Quantitative MRI Measures of Tissue Injury

Eight out of ten qMRI metrics showed the same direction of differences in ASCC as previously seen in DCM (p=0.11), including significant differences in five metrics: increased T2*WI WM/GM at all levels (rostral: p=0.03, MCL: p=0.005, caudal: p=0.01), decreased MCL FA (p=0.04), and decreased rostral MTR (p=0.046) (Table 3). CSA measures varied in the opposite direction from DCM, including significantly higher rostral CSA in ASCC (p=0.02). Ratios of MCL:rostral qMRI metrics showed trends toward decreased FA ratio (p=0.06) and CSA ratio (p=0.09) in ASCC subjects (Table 4).

Table 3: Comparison of Normalized Quantitative MRI Metrics. Normalized MRI metrics were compared between subjects with and without cord compression. A composite Z score was used as an overall measure of tissue injury. Data extracted at the MCL were converted to Z scores to normalize for rostrocaudal variations prior to comparison and then converted back to values at C4-5 for convenience of interpretation. The direction of differences were compared to findings in DCM patients compared to asymptomatic subjects. Caudal CSA and MTR were not analyzed because they did not show significant results in our prior DCM study.[15] * denotes significance (p<0.05).

Region	MRI Metric	Uncompressed (N=20)	Compressed (N=20)	P Value	Direction Matches DCM
Rostral (C1-C3)	CSA	75.4 ± 4.7	81.7 ± 9.6	0.02**	N
	FA	0.731 ± 0.031	0.720 ± 0.037	0.48	Y
	MTR	53.6 ± 3.0	51.9 ± 1.8	0.046**	Y
	T2*WI WM/GM	0.838 ± 0.029	0.863 ± 0.031	0.03**	Y
Mid (MCL or C4-5)	CSA	79.2 ± 7.7	81.9 ± 12.8	0.34	N
	FA	0.670 ± 0.044	0.631 ± 0.043	0.04**	Y
	MTR	51.1 ± 3.3	49.8 ± 2.4	0.35	Y
	T2*WI WM/GM	0.842 ± 0.019	0.864 ± 0.026	0.005**	Y
Caudal (C6-C7)	FA	0.616 ± 0.046	0.595 ± 0.051	0.24	Y
	T2*WI WM/GM	0.845 ± 0.037	0.881 ± 0.050	0.01**	Y
Composite Score		0 ± 1	-0.984 ± 1.259	0.002**	Y

Table 4: Comparison of Metric Ratios. Ratios were calculated by dividing MCL metric values by rostral values. * denotes trend (p<0.10) and ** denotes significance (p<0.05).

MCL: Rostral Ratio	Uncompressed (N=20)	Compressed (N=20)	P Value
CSA	1.050 ± 0.060	1.003 ± 0.106	0.09*
FA	0.917 ± 0.054	0.878 ± 0.056	0.06*
MTR	0.954 ± 0.042	0.960 ± 0.033	0.56
T2*WI WM/GM	1.005 ± 0.029	1.001 ± 0.025	0.67

Multivariate Results

The qMRI composite score showed stronger differences than single metrics (p=0.002; Table 3), including abnormal results (t_{10} score < -2.23) in 6/20 compressed subjects (Figure 3). Replacing CSA measures with CSA ratio, a revised composite score showed even stronger results ($p=8x10^{-5}$), including 9/20 compressed subjects with abnormal results (t_9 score < -2.26; Figure 3). A logistic regression model retaining MCL T2*WI WM/GM (p=0.006), FA ratio (p=0.06), CSA ratio (p=0.11), and rostral MTR (p=0.34) yielded discrimination of 0.941 between compressed and uncompressed subjects ($p=2x10^{-5}$).

Tissue Injury by Anatomical Structure

Compressed subjects had decreased FA and MTR in the VCs (p=0.01, 0.02, respectively), while the LCs, DCs, and GM did not show significant differences in these metrics (Figure 4). In contrast, T2*WI WM/GM was increased in the LCs and DCs (p=0.009, 0.0004, respectively) in compressed subjects, while the VCs showed no difference.

Clinical Follow-up

All 20 ASCC subjects had follow-up assessments (median: 21 months, range: 3-27 months). Four subjects reported concerning new symptoms, and following physical examination two were diagnosed with DCM (10%, 95% CI: 1.8-33.1%) and referred for surgical consultation. One experienced neck pain, intermittent right hand numbness, and gait imbalance (mJOA=17), and examination showed marked gait ataxia, asymmetric hyperreflexia, and positive left Hoffman sign. The other had neck pain, left hand numbness, and mild gait instability (mJOA=16), and examination revealed symmetric hyperreflexia and mild gait ataxia. This individual sought medical attention with her family physician, but no diagnosis was made after a new MRI was reported as “normal degenerative changes”.

Prediction of Symptomatic Myelopathy Development

Demographic variables and baseline qMRI metrics were not predictive of myelopathy development in univariate or multivariate analyses.

Discussion

Summary of Findings

This study establishes an objective definition of SC compression and finds that asymptomatic compression is common, affecting approximately half of healthy adults and increasing in frequency with age. Multiparametric quantitative MRI provides compelling evidence that ASCC involves a mild degree of SC tissue injury. Significant differences were found with five qMRI metrics (rostral, MCL, and caudal T2*WI WM/GM, rostral MTR, and MCL FA), with T2*WI WM/GM and MTR results suggesting that demyelination is the predominant pathophysiological mechanism in this preclinical state.[12,13,19] The finding of decreased MCL FA confirms two previous reports,[18,20] and may be indicative of axonal injury but could alternatively be related to demyelination.[21] However, this result could be artifactual, as DTI metrics can be biased in the compressed SC by increased susceptibility artefact,[12,21] and thus it was reassuring that other measures showed changes away from the compressed

region. Furthermore, the study by Lindberg et al. (2016) included only five ASCC subjects, who showed functional deficits, while the Kerkovsky et al. (2012) study included subjects with radiculopathy, which can localize within the SC GM (i.e. myeloradiculopathy). In contrast, our cohort was carefully screened to ensure the absence of neurological symptoms and signs. Recently, a larger study was completed with 92 ASCC and 71 uncompressed subjects, but DTI differences between these groups were not reported.[22] Our finding that rostral CSA was significantly greater among ASCC subjects suggests that atrophy does not occur in this condition, but rather, having a larger SC is a predisposing factor for compression, in keeping with a prior report that investigated SC occupation ratio.[7] MCL CSA was also (non-significantly) larger in uncompressed subjects, but the ratio of MCL to rostral CSA showed a trend toward a decrease in ASCC, indicating that compression has a minor effect on CSA and normalization by rostral values helps to mitigate the high inter-subject variability of this measure.[7,14] Although the groups with and without cord compression differed significantly in age and weight, all qMRI metrics were corrected for age and none showed significant variation with weight. In fact, MTR and FA have previously been shown to vary with age,[11,14] but these relationships became non-significant when compression was included in the analysis, confirming a recent DTI study,[22] suggesting that earlier studies overestimated the effect of age.[14,23,24] SC compression was primarily anterior in all subjects, and this appeared to preferentially cause injury to the VCs, as measured by reduced FA and MTR. T2*WI WM/GM demonstrated conflicting results with significant changes in LCs and DCs and no significant effect in the VCs; we suspect that this is attributable to ventral artifacts on T2*WI, including chemical shift at the CSF-cord interface and blooming artefact from prominent anterior veins, but histopathological correlation is required. The GM did not show significant differences for FA or MTR, which is likely a limitation of these metrics as they are better at detecting WM pathology.[12] Follow-up clinical data showed development of clinical myelopathy in 10% of subjects, similar to a prior report,[10] indicating that ASCC is a meaningful preclinical condition. Prediction of myelopathy development was not successful given the small ASCC sample and number of events, but further investigation is warranted to identify prognostic factors.

Our results highlight the value of multiparametric qMRI and multivariate analysis; the combination of multiple tissue injury measures into composite scores reduces the standard error of effect estimation by approximately $1/\sqrt{n}$, revealing robust group differences. Post hoc analysis identified an even greater effect of compression, with the revised composite score finding abnormal results in nine ASCC subjects, and logistic regression results suggesting that the vast majority with ASCC experience tissue injury. However, such data-driven analysis may suffer from overfitting and must be interpreted with caution. In fact, without histopathological studies, the ground truth is unknown regarding microstructural changes that occur in ASCC, and to our knowledge no cadaver studies have investigated this topic. Overall, the results support our hypothesis at a group level, indicating that SC tissue injury occurs in subjects with only a mild degree of compression who lack any manifestation of clinical symptoms or signs. This offers the intriguing possibility of diagnosing SC tissue injury prior to the onset of neurological impairment in this condition and others, with far-reaching clinical implications.

An Objective Definition of Spinal Cord Compression

The prevalence estimates in our data are similar to the range of 51.5-66.2% (for age 40-80) reported by Kovalova et al. (2016),[8] but far higher than earlier reports of 8-26%.[3-7] These differences are primarily due to vague and subjective definitions of SC compression in prior

studies, which used the terms impingement, encroachment, and compression without strict criteria.[3-7] Kerkovsky et al. (2012) provided a more precise definition of SC compression: a concave defect adjacent to a bulging disc or osteophyte and/or CR < 0.4;[18] however, their threshold for CR was very low, at 4.5 SDs below the mean (based on our normative data at C5-6) and did not account for normal variations of CR across levels. Furthermore, the error associated with manual CR measurement has not been characterized, and visual assessment of concavity is subjective. Kovalova et al. (2016) provided detailed descriptions of indentation, flattening, and circumferential compression, but did not establish quantitative criteria.[8] Instead, we use automated analysis to reduce bias and define SC compression as deviation from normal SC morphology in 3 quantitative parameters that reflect flattening, indentation, and torsion (due to lateral bulging discs). This approach identified four levels of subtle compression missed by two expert raters and achieved diagnostic accuracy approaching 100%. 2D PCA readily detects the transverse axis of the SC, allowing calculation of CR and relative rotation, while indentation is robustly calculated using convex hulls. Several additional shape parameters are also under investigation including asymmetry indices to detect lateral compression and relative CSA to detect circumferential compression, but these were not necessary in this cohort. Automatic analysis is fast and straightforward using the free open-source Spinal Cord Toolbox,[16] and the only manual step is reviewing and editing the segmentation. Our results define normative data for each shape parameter across cervical intervertebral levels, and ROC analysis identified diagnostic thresholds that were close to 2 SDs from the mean of each metric. Many of our ASCC cases showed CSF intervening between the compressive process (e.g. disc osteophyte complex) and the ventral spinal cord surface, as the SC shifts posteriorly when the subject is supine. This indicates that the cord deformity is observed in the absence of visible compression, suggesting that shape analysis can detect dynamic SC compression, which has previously only been possible with flexion/extension MRI.[25]

Contemplating the Definition of Myelopathy

Dictionaries typically define myelopathy as “a disease or disorder of the spinal cord”, and our results suggest that individuals with ASCC meet this description. In contrast, clinicians have historically favoured functional criteria: the presence of neurological symptoms and signs that localize to the SC.[26] This clinical definition most likely originated due to the lack of diagnostic investigations that can accurately detect early pathological changes within the cord. It appears that symptoms and signs of myelopathy only emerge once a considerable degree of tissue injury occurs, and homeostatic mechanisms of neuroplasticity and behavioural adaptation may mask early changes. Technological advances have led to the emergence of *in vivo* diagnostic tools, including qMRI, that have the potential to surpass clinical assessments by taking direct measurements from the SC. Similar progress has been made in electrophysiology with the development of contact heat evoked potentials (CHEPs),[27] which appear to be more sensitive than motor and sensory evoked potentials for myelopathy.[18] As these tools become more sophisticated and refined, they will allow progressively earlier detection of tissue injury in this condition, in which the ground truth likely constitutes a continuum between normal and abnormal without a clear division, similar to degenerative processes in the aging brain.

Clinical Implications

Our results suggest that the widely held paradigm – that mild SC indentation and flattening represent “normal degenerative changes” – is incorrect. Rather, ASCC represents a highly

prevalent preclinical diagnosis with microstructural tissue changes, akin to the pre-diabetic state of insulin resistance, and these patients are at risk for progression to clinical myelopathy. A prior study found that 8% of individuals with ASCC experience progression to symptomatic myelopathy at 1 year and 22.6% at 4 years, with risk factors including presence of radiculopathy, T2WI hyperintensity, or prolonged conduction on electrophysiology studies.[10] Thus, individuals with ASCC should be educated about myelopathy symptoms periodically examined by a clinician. Unfortunately, patients often ignore early neurological symptoms, as was evident in two excluded subjects with evidence of mild DCM, of which they were not aware. Furthermore, primary care clinicians sometimes miss the diagnosis of DCM, as in one of our ASCC subjects that developed myelopathy, or diagnose it only after debilitating symptoms have developed, at which point surgical treatment rarely restores normal ambulation and hand function. Earlier diagnosis of DCM would allow earlier treatment, and surgery is associated with reduced morbidity in all severity categories including mild DCM.[28] Preliminary results suggest that serial qMRI assessments may also be helpful in detecting progression of tissue injury [29], and long-term clinical and qMRI monitoring of this cohort of ASCC subjects is planned. Multiparametric qMRI may also hold potential for earlier diagnosis of other spinal conditions, which share pathophysiological mechanisms of demyelination, axonal injury, gliosis, and atrophy.[13]

Limitations

The sample size was large enough to demonstrate the presence of tissue injury in ASCC, but larger studies are needed to provide more accurate estimates of prevalence and rate of myelopathy development. Our normalization approach for age and other subject characteristics may be inaccurate, and ideally groups would be matched for these variables (although this is difficult because ASCC is age-related and its presence is typically unknown at time of recruitment). Quantitative shape analysis is dependent on an accurate SC segmentation, and manual editing of segmentations was necessary in most subjects. Automatic segmentation of the compressed SC is challenging due to anatomical distortion and reduced contrast with surrounding tissues, and alternative approaches are under investigation by the SCT developers. Shape analysis would be enhanced by using an optimized high-resolution T2WI acquisition, but our T2WI had only moderate resolution and frequently showed motion artifacts.

Conclusions

ASCC is a common age-related preclinical state that can be accurately and objectively diagnosed with automated analysis of SC morphology. This condition involves a similar pattern of macro- and microstructural changes as symptomatic DCM, representing subclinical tissue injury, and individuals with ASCC at an increased risk of myelopathy development. These results have important clinical implications, including the need to educate and monitor ASCC subjects for symptoms and signs of myelopathy, while offering the possibility of presymptomatic diagnosis and treatment of other spinal pathologies.

Author Contributions

All authors provided final approval of this manuscript to be published. All authors agreed to be accountable for all aspects of the work.

Allan R. Martin: Primary contributor to study conception, design, clinical examinations of subjects, MRI data collection, image analysis, statistical analysis, and manuscript writing. This study was part of Dr. Martin's PhD thesis work at University of Toronto.

Benjamin De Leener: Contributed to study design, MRI data collection, image analysis, spinal cord shape analysis, statistical analysis, and manuscript editing.

Julien Cohen-Adad: Contributed to study design, MRI data collection, image analysis, spinal cord shape analysis, statistical analysis, and manuscript editing.

David W. Cadotte: Contributed to study design, statistical analysis, and manuscript editing.

Aria Nouri: Contributed to study design, clinical examinations, MRI data collection, image analysis, statistical analysis, and manuscript editing.

Jefferson R. Wilson: Contributed to statistical analysis, and manuscript editing.

Lindsay Tetreault: Contributed to MRI data collection, statistical analysis, and manuscript editing.

Adrian Crawley: Contributed to study design, statistical analysis, and manuscript editing.

David J. Mikulis: Contributed to study design, statistical analysis, and manuscript editing.

Howard Ginsberg: Contributed to study design, statistical analysis, and manuscript editing.

Michael G. Fehlings: Senior author and PhD supervisor to Dr. Martin. Contributed to study conception, design, statistical analysis, and manuscript editing.

References

1. Nouri A, Tetreault L, Singh A, Karadimas SK, Fehlings MG. Degenerative Cervical Myelopathy: Epidemiology, Genetics, and Pathogenesis. Spine (Phila Pa 1976) 2015;40:E675-93.
2. Kalsi-Ryan S, Karadimas SK, Fehlings MG. Cervical spondylotic myelopathy: the clinical phenomenon and the current pathobiology of an increasingly prevalent and devastating disorder. Neuroscientist 2013;19:409-21.
3. Teresi LM, Lufkin RB, Reicher MA, et al. Asymptomatic degenerative disk disease and spondylosis of the cervical spine: MR imaging. Radiology 1987;164:83-8.
4. Boden SD, McCowin PR, Davis DO, Dina TS, Mark AS, Wiesel S. Abnormal magnetic-resonance scans of the cervical spine in asymptomatic subjects. A prospective investigation. J Bone Joint Surg Am 1990;72:1178-84.
5. Matsumoto M, Fujimura Y, Suzuki N, et al. MRI of cervical intervertebral discs in asymptomatic subjects. J Bone Joint Surg Br 1998;80:19-24.
6. Lee MJ, Cassinelli EH, Riew KD. Prevalence of cervical spine stenosis. Anatomic study in cadavers. J Bone Joint Surg Am 2007;89:376-80.
7. Kato F, Yukawa Y, Suda K, Yamagata M, Ueta T. Normal morphology, age-related changes and abnormal findings of the cervical spine. Part II: Magnetic resonance imaging of over 1,200 asymptomatic subjects. Eur Spine J 2012;21:1499-507.
8. Kovalova I, Kerkovsky M, Kadanka Z, et al. Prevalence and Imaging Characteristics of Nonmyelopathic and Myelopathic Spondylotic Cervical Cord Compression. Spine (Phila Pa 1976) 2016;41:1908-16.
9. Bartlett RJ, Hill CA, Rigby AS, Chandrasekaran S, Narayanamurthy H. MRI of the cervical spine with neck extension: is it useful? Br J Radiol 2012;85:1044-51.
10. Bednarik J, Kadanka Z, Dusek L, et al. Presymptomatic spondylotic cervical myelopathy: an updated predictive model. Eur Spine J 2008;17:421-31.
11. Martin AR, Aleksanderek I, Cohen-Adad J, et al. Translating state-of-the-art spinal cord MRI techniques to clinical use: A systematic review of clinical studies utilizing DTI, MT, MWF, MRS, and fMRI. Neuroimage Clin 2016;10:192-238.
12. Stroman PW, Wheeler-Kingshott C, Bacon M, et al. The current state-of-the-art of spinal cord imaging: Methods. Neuroimage 2014;84:1070-81.
13. Wheeler-Kingshott CA, Stroman PW, Schwab JM, et al. The current state-of-the-art of spinal cord imaging: Applications. Neuroimage 2014;84:1082-93.
14. Martin AR, De Leener B, Cohen-Adad J, et al. Clinically feasible microstructural MRI to quantify cervical spinal cord tissue injury using DTI, MT, and T2*-weighted imaging: assessment of normative data and reliability. AJNR 2017;In press.
15. Martin AR, De Leener B, Cohen-Adad J, et al. A Novel MRI Biomarker of Spinal Cord White Matter Injury: T2*-weighted White Matter to Grey Matter Signal Intensity Ratio. AJNR 2017;In press.
16. De Leener B, Levy S, Dupont SM, et al. SCT: Spinal Cord Toolbox, an open-source software for processing spinal cord MRI data. Neuroimage 2017;145:24-43.
17. Kameyama T, Hashizume Y, Ando T, Takahashi A. Morphometry of the normal cadaveric cervical spinal cord. Spine (Phila Pa 1976) 1994;19:2077-81.
18. Kerkovsky M, Bednarik J, Dusek L, et al. Magnetic resonance diffusion tensor imaging in patients with cervical spondylotic spinal cord compression: correlations between clinical and electrophysiological findings. Spine (Phila Pa 1976) 2012;37:48-56.
19. Cohen-Adad J. What can we learn from T2* maps of the cortex? Neuroimage 2014;93 Pt 2:189-200.

20. Lindberg PG, Sanchez K, Ozcan F, et al. Correlation of force control with regional spinal DTI in patients with cervical spondylosis without signs of spinal cord injury on conventional MRI. Eur Radiol 2016;26:733-42.
21. Cohen-Adad J, El Mendili MM, Lehericy S, et al. Demyelination and degeneration in the injured human spinal cord detected with diffusion and magnetization transfer MRI. Neuroimage 2011;55:1024-33.
22. Kerkovsky M, Bednarik J, Jurova B, et al. Spinal Cord MR Diffusion Properties in Patients with Degenerative Cervical Cord Compression. J Neuroimaging 2017;27:149-57.
23. Mamata H, Jolesz FA, Maier SE. Apparent diffusion coefficient and fractional anisotropy in spinal cord: Age and cervical spondylosis-related changes. J Magn Reson Imaging 2005;22:38-43.
24. Taso M, Girard OM, Duhamel G, et al. Tract-specific and age-related variations of the spinal cord microstructure: a multi-parametric MRI study using diffusion tensor imaging (DTI) and inhomogeneous magnetization transfer (ihMT). Nmr Biomed 2016;29:817-32.
25. Nouri A, Martin AR, Mikulis DJ, Fehlings MG. Magnetic resonance imaging assessment of degenerative cervical myelopathy: A review of structural changes and measurement techniques. Neurosurgical Focus 2016;40:E5.
26. Seidenwurm DJ, Expert Panel on Neurologic I. Myelopathy. AJNR Am J Neuroradiol 2008;29:1032-4.
27. Jutzeler C, Ulrich A, Huber B, Rosner J, Kramer J, Curt A. Improved diagnosis of cervical spondylotic myelopathy with contact heat evoked potentials. J Neurotrauma 2017.
28. Fehlings MG, Wilson JR, Kopjar B, et al. Efficacy and safety of surgical decompression in patients with cervical spondylotic myelopathy: results of the AOSpine North America prospective multi-center study. J Bone Joint Surg Am 2013;95:1651-8.
29. Martin AR, De Leener B, Cohen-Adad J, et al. Toward Clinical Translation of Quantitative Spinal Cord MRI: Serial Monitoring to Identify Disease Progression in Patients with Degenerative Cervical Myelopathy. International Society for Magnetic Resonance in Medicine. Honolulu, Hawaii, USA2017.

Figure Captions

Figure 1: Automatic Shape Analysis. T2*WI of asymptomatic subjects showing flattening (A), indentation (B), and torsion (C) of the SC. D: the SC segmentation (red) is analyzed with 2D PCA to identify the long (transverse) and short (AP) axes (green) that intersect at the centre of mass, and CR is calculated as ratio of AP to transverse diameters to measure flattening. E: a convex hull (green) is computed that surrounds the segmentation (red), and solidity is calculated as the ratio of segmented area to subtended area. F: the angle between the transverse axis and horizontal is computed, and then relative rotation is calculated as the ratio between the current slice and average angle in slices above and below.

Figure 2: Frequency of ASCC by Decade. The frequency of ASCC is plotted against decade of life, with data for each decade provided in parentheses. ASCC: asymptomatic spinal cord compression.

Figure 3: Distributions of Composite Scores. Top: histograms (bars) of composite scores (average of the z scores of 10 qMRI metrics) are displayed for subjects with ASCC (red) and no cord compression (blue). The expected distribution of results based on the null hypothesis (t distribution with ten d.f.s) is superimposed. Six ASCC subjects had abnormally low composite score ($t_{10} < -2.23$) and group differences were significant (Wilcoxon test: p=0.002). Bottom: the same plot is displayed for a revised composite score that replaces rostral and MCL CSA measures with CSA ratio (selected post hoc), and the corresponding t distribution with nine degrees of freedom. Nine ASCC subjects had abnormal scores ($t_9 < -2.26$) and stronger group differences were found (p=0.00008).

Figure 4: Quantitative MRI Metrics by Anatomical Structure. Images include a FA map (A), a MTR map (B), and a T2*-weighted image (C) of C3-4 in an uncompressed subject. Panels D-F show the SCT probabilistic maps of the VCs (yellow), LCs (blue), DCs (red), and GM (green) overlaid. DCs: dorsal columns, FA: fractional anisotropy, GM: grey matter, LCs: lateral columns, MTR: magnetization transfer ratio, SCT: Spinal Cord Toolbox, VCs: ventral columns.

Supplemental Tables

Supplemental Table 1: Anatomical Features of Spinal Cord Compression and Quantitative Shape Metrics. MRI images were analyzed for degenerative changes causing cervical spinal cord compression, defined as indentation, flattening, or focal torsion. Levels with cord compression are listed with CR in parentheses, and a description of the degenerative changes and morphology of cord compression are provided. ASCC: asymptomatic spinal cord compresison, CR: compression ratio, DOC: disc ± osteophyte complex, LF: ligamentum flavum, MCL: maximally compressed level, RR: relative rotation, Sol.: solidity.

#	Age, Sex	MCL	Comp. Levels	CR (%)	Sol. (%)	RR (°)	MRI Features
1	74M	C5-6	C4-5	51.5*	95.8	-1.4	Broad DOC flattening cord
			C5-6	49.3*	96.4	0.3	Broad DOC flattening cord
			C6-7	48.6*	95.2	-2.3	Lateral DOC flattening and rotating cord
2	55F	C3-4	C3-4	53.1*	93.9*	-1.0	Central DOC indenting and flattening cord, mild LF hypertrophy
			C4-5	51.7*	94.6*	-0.7	Central DOC indenting and flattening cord, mild LF hypertrophy
3	59F	C5-6	C3-4	47.8*	95.3*	1.3	Broad DOC flattening and indenting cord
			C4-5	48.5*	96.1	0.5	Broad DOC flattening cord
			C5-6	45.6*	98.2	0.5	Broad DOC flattening cord
4	28M	C4-5	C3-4	57.8	95.4*	-1.2	Central DOC indenting cord
			C4-5	53.4	94.4*	-1.0	Central DOC indenting cord
			C5-6	51.7	95.4*	-1.4	Central DOC indenting cord
5	30M	C5-6	C5-6	55.4	94.6*	2.1	Central DOC indenting cord
			C6-7	53.9	93.9*	2.1	Central DOC indenting cord
6	52F	C4-5	C3-4	56.4	94.3*	-1.8	Central DOC indenting cord, mild LF hypertrophy at C3-4, C4-5
			C4-5	60.8	92.7*	-2.9	Central DOC indenting cord, mild LF hypertrophy
			C5-6	61.1	95.4*	-7.0*	Lateral DOC indenting and rotating cord
			C6-7	48.6*	93.8*	1.0	Central DOC indenting and flattening cord
7	60F	C5-6	C5-6	50.4*	95.4*	0.7	Broad DOC flattening cord
8	69M	C5-6	C5-6	48.9*	97.5	-0.7	Broad DOC flattening cord
			C6-7	49.0*	95.8	2.5	Broad DOC flattening cord
9	66F	C4-5	C4-5	55.4	94.2*	0.0	Central DOC indenting cord, mild LF hypertrophy
10	51M	C6-7	C6-7	43.4*	91.6*	-0.9	Central DOC indenting and flattening cord
11	39M	C6-7	C6-7	55.4	94.7*	4.5*	Lateral DOC indenting and rotating cord
12	49M	C6-7	C4-5	55.2	93.7*	-0.2	Central DOC indenting cord
			C5-6	49.5*	95.8	2.1	Broad DOC flattening cord
			C6-7	46.1*	92.9*	-5.0*	Lateral DOC indenting, flattening, and rotating cord
13	50F	C5-6	C4-5	55.5	94.1*	0.5	Central DOC indenting cord
			C5-6	55.0	95.3*	-4.2*	Broad lateral DOC indenting and rotating cord
14	51F	C4-5	C3-4	55.8	95.4*	-0.8	Central DOC indenting cord
			C4-5	54.0	93.0*	1.9	Central DOC indenting cord
			C5-6	54.3	95.6	0.6	Central DOC indenting cord
15	55F	C4-5	C3-4	46.9*	96.2	0.8	Broad DOC flattening cord
			C4-5	41.3*	95.4*	0.6	Central DOC indenting cord
			C5-6	42.0*	96.0	-0.4	Broad DOC flattening cord
16	79F	C5-6	C4-5	52.3	95.5*	-1.3	Central DOC indenting cord
			C5-6	46.7*	93.3*	-2.0	Central DOC indenting and flattening cord
17	77M	C5-6	C3-4	53.2*	92.8*	-4.0*	Lateral DOC indenting and rotating cord
			C4-5	48.6*	95.8	-0.4	Broad central DOC flattening cord

			C5-6	48.3*	93.9*	-2.9*	Broad DOC indenting, flattening, and rotating cord
18	44M	C5-6	C3-4	55.6	94.9*	-0.7	Central DOC indenting cord
			C4-5	55.7	95.1*	1.4	Central DOC indenting cord
			C5-6	45.4*	93.4*	0.0	Central DOC indenting and flattening cord, mild LF hypertrophy
19	56M	C5-6	C5-6	53.6	94.8*	-1.3	Circumferential compression, flattening from broad DOC and LF hypertrophy
20	54M	C6-7	C4-5	51.5	95.3*	0.1	Central DOC indenting cord
			C6-7	46.6*	96.7	-2.4*	Broad DOC flattening and rotating cord

Supplemental Table 2: Variations of MRI Measures with Subject Characteristics. The relationship between qMRI metrics and subject characteristics (age, sex, height, weight, and cervical cord length) were analyzed with backward stepwise multiple linear regression that also included a binary independent variable for the presence of cord compression. Age was retained in each model regardless of significance, and linear coefficients for age and any other significant relationships (CSA with cervical cord length and MTR with height) were subsequently used to normalize qMRI metrics.

Region	MRI Metric	Age	Sex	Height	Weight	Cervical Cord Length
Rostral (C1-C3)	CSA	β=-0.168 (p=0.10)	-	-	-	β=4.81 (p=0.002)
	FA	$\beta=-6.06\times10^{-4}$ (p=0.19)	-	-	-	-
	MTR	β=-0.0472 (p=0.13)	-	β=-0.181 (p=0.0004)	-	-
	T2*WI WM/GM	$\beta=2.34\times10^{-4}$ (p=0.53)	-	-	-	-
MCL or C4-5	CSA	β=-0.195 (p=0.17)	-	-	-	β=4.90 (p=0.02)
	FA	$\beta=-7.16\times10^{-4}$ (p=0.22)	-	-	-	-
	MTR	β=-0.0545 (p=0.15)	-	β=-0.146 (p=0.01)	-	-
	T2*WI WM/GM	$\beta=3.39\times10^{-5}$ (p=0.91)	-	-	-	-
Caudal (C6-C7)	FA	β=-0.00127 (p=0.12)	-	-	-	-
	T2*WI WM/GM	$\beta=1.20\times10^{-4}$ (p=0.83)	-	-	-	-

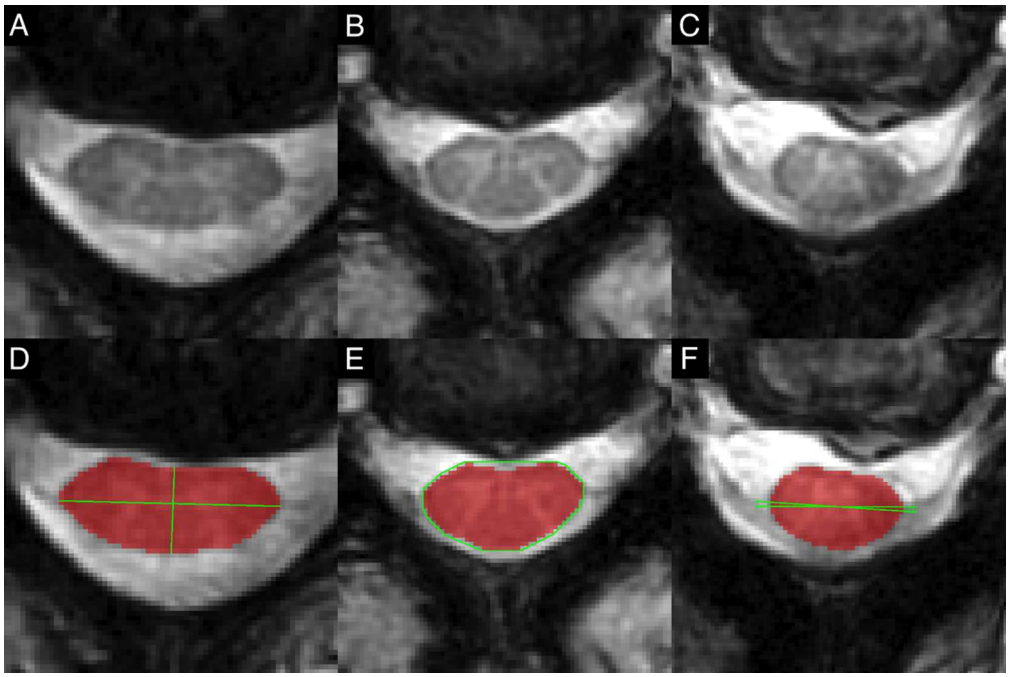

Figure 1: Automatic Shape Analysis. T2*WI of asymptomatic subjects showing flattening (A), indentation (B), and torsion (C) of the SC. D: the SC segmentation (red) is analyzed with 2D PCA to identify the long (transverse) and short (AP) axes (green) that intersect at the centre of mass, and CR is calculated as ratio of AP to transverse diameters to measure flattening. E: a convex hull (green) is computed that surrounds the segmentation (red), and solidity is calculated as the ratio of segmented area to subtended area. F: the angle between the transverse axis and horizontal is computed, and then relative rotation is calculated as the ratio between the current slice and average angle in slices above and below.

101x67mm (300 x 300 DPI)

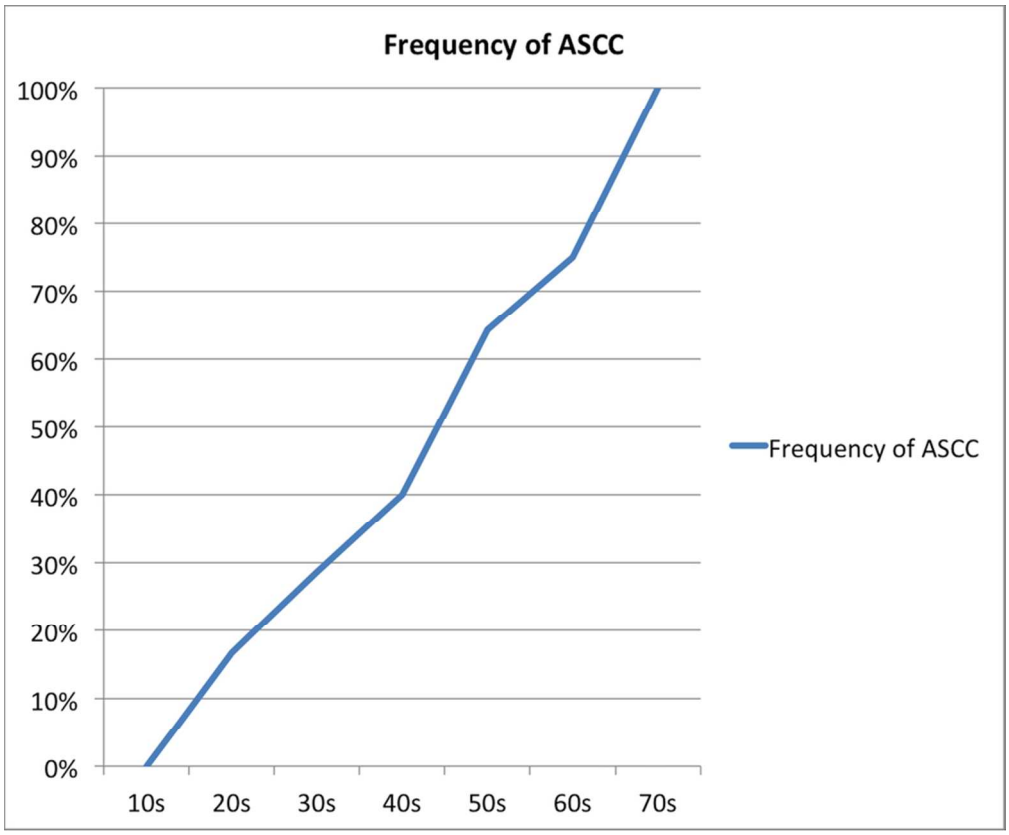

Figure 2: Frequency of ASCC by Decade. The frequency of ASCC is plotted against decade of life, with data for each decade provided in parentheses. ASCC: asymptomatic spinal cord compression.

84x69mm (300 x 300 DPI)

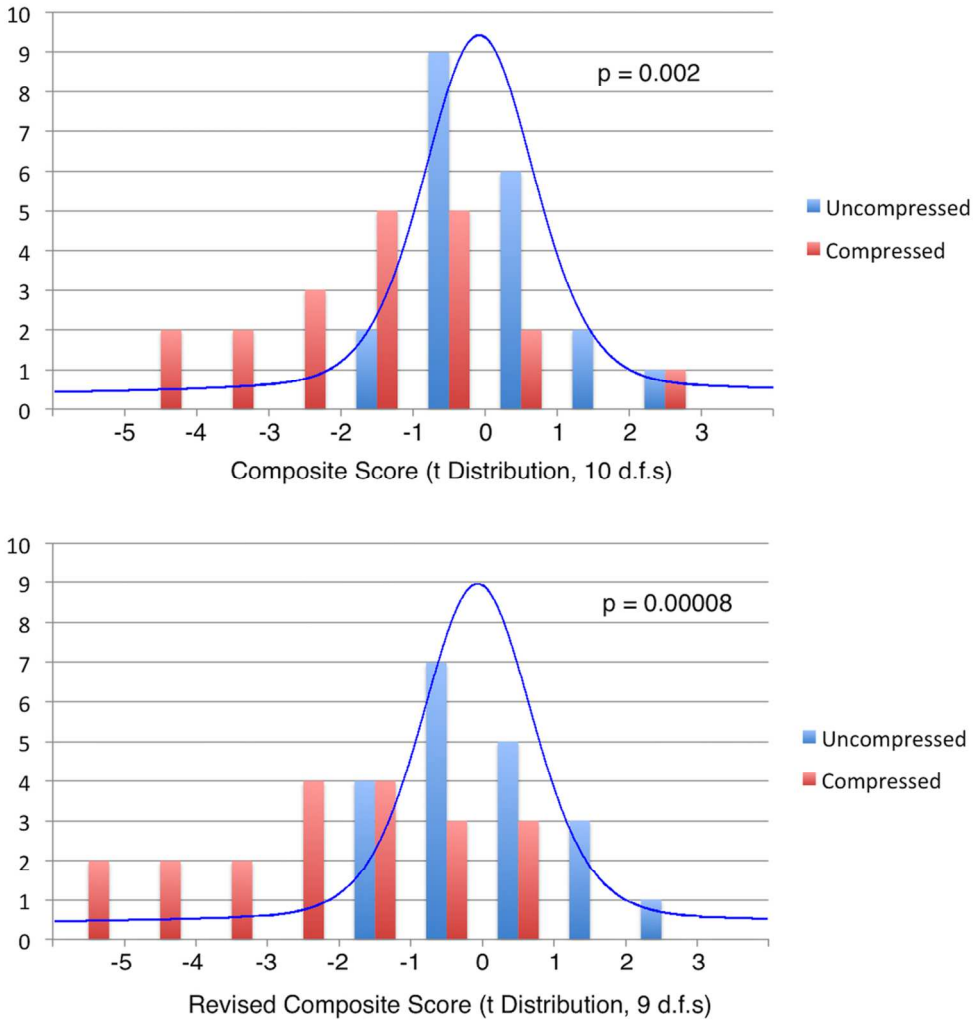

Figure 3: Distributions of Composite Scores. Top: histograms (bars) of composite scores (average of the z scores of 10 qMRI metrics) are displayed for subjects with ASCC (red) and no cord compression (blue). The expected distribution of results based on the null hypothesis (t distribution with ten d.f.s) is superimposed. Six ASCC subjects had abnormally low composite score (t10 < -2.23) and group differences were significant (Wilcoxon test: p=0.002). Bottom: the same plot is displayed for a revised composite score that replaces rostral and MCL CSA measures with CSA ratio (selected post hoc), and the corresponding t distribution with nine degrees of freedom. Nine ASCC subjects had abnormal scores (t9 < -2.26) and stronger group differences were found (p=0.00008).

111x120mm (300 x 300 DPI)

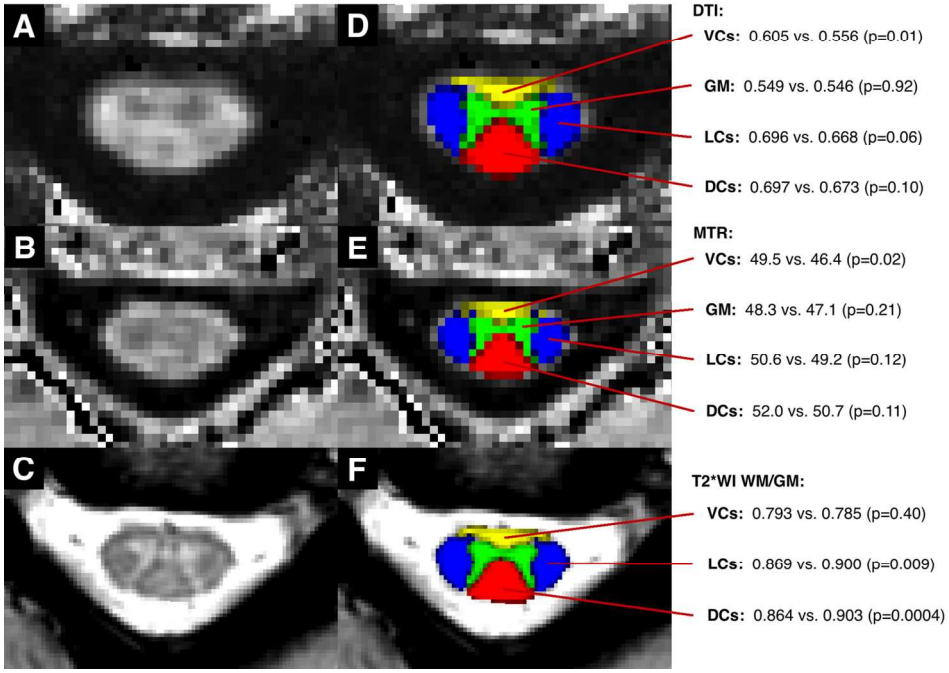

Figure 4: Quantitative MRI Metrics by Anatomical Structure. Images include a FA map (A), a MTR map (B), and a T2*-weighted image (C) of C3-4 in an uncompressed subject. Panels D-F show the SCT probabilistic maps of the VCs (yellow), LCs (blue), DCs (red), and GM (green) overlaid. DCs: dorsal columns, FA: fractional anisotropy, GM: grey matter, LCs: lateral columns, MTR: magnetization transfer ratio, SCT: Spinal Cord Toolbox, VCs: ventral columns.

139x102mm (300 x 300 DPI)

STROBE Statement—checklist of items that should be included in reports of observational studies

	Item No	Recommendation	Page
Title and abstract	1	(*a*) Indicate the study's design with a commonly used term in the title or the abstract	2
		(*b*) Provide in the abstract an informative and balanced summary of what was done and what was found	2
Introduction			
Background/rationale	2	Explain the scientific background and rationale for the investigation being reported	4
Objectives	3	State specific objectives, including any prespecified hypotheses	4
Methods			
Study design	4	Present key elements of study design early in the paper	4-5
Setting	5	Describe the setting, locations, and relevant dates, including periods of recruitment, exposure, follow-up, and data collection	4-5
Participants	6	(*a*) *Cohort study*—Give the eligibility criteria, and the sources and methods of selection of participants. Describe methods of follow-up *Case-control study*—Give the eligibility criteria, and the sources and methods of case ascertainment and control selection. Give the rationale for the choice of cases and controls *Cross-sectional study*—Give the eligibility criteria, and the sources and methods of selection of participants	4-5 N/A N/A
		(*b*) *Cohort study*—For matched studies, give matching criteria and number of exposed and unexposed *Case-control study*—For matched studies, give matching criteria and the number of controls per case	N/A N/A
Variables	7	Clearly define all outcomes, exposures, predictors, potential confounders, and effect modifiers. Give diagnostic criteria, if applicable	5-6
Data sources/ measurement	8*	For each variable of interest, give sources of data and details of methods of assessment (measurement). Describe comparability of assessment methods if there is more than one group	4-6
Bias	9	Describe any efforts to address potential sources of bias	12
Study size	10	Explain how the study size was arrived at	13
Quantitative variables	11	Explain how quantitative variables were handled in the analyses. If applicable, describe which groupings were chosen and why	5-6
Statistical methods	12	(*a*) Describe all statistical methods, including those used to control for confounding	6
		(*b*) Describe any methods used to examine subgroups and interactions	6
		(*c*) Explain how missing data were addressed	4
		(*d*) *Cohort study*—If applicable, explain how loss to follow-up was addressed *Case-control study*—If applicable, explain how matching of cases and controls was addressed *Cross-sectional study*—If applicable, describe analytical methods taking account of sampling strategy	N/A N/A N/A
		(*e*) Describe any sensitivity analyses	N/A

Continued on next page

			Page
Results			
Participants	13*	(a) Report numbers of individuals at each stage of study—eg numbers potentially eligible, examined for eligibility, confirmed eligible, included in the study, completing follow-up, and analysed	7-10
		(b) Give reasons for non-participation at each stage	7-10
		(c) Consider use of a flow diagram	N/A
Descriptive data	14*	(a) Give characteristics of study participants (eg demographic, clinical, social) and information on exposures and potential confounders	7
		(b) Indicate number of participants with missing data for each variable of interest	N/A
		(c) *Cohort study*—Summarise follow-up time (eg, average and total amount)	7-10
Outcome data	15*	*Cohort study*—Report numbers of outcome events or summary measures over time	7-10
		Case-control study—Report numbers in each exposure category, or summary measures of exposure	N/A
		Cross-sectional study—Report numbers of outcome events or summary measures	N/A
Main results	16	(*a*) Give unadjusted estimates and, if applicable, confounder-adjusted estimates and their precision (eg, 95% confidence interval). Make clear which confounders were adjusted for and why they were included	7-10
		(*b*) Report category boundaries when continuous variables were categorized	N/A
		(*c*) If relevant, consider translating estimates of relative risk into absolute risk for a meaningful time period	N/A
Other analyses	17	Report other analyses done—eg analyses of subgroups and interactions, and sensitivity analyses	N/A
Discussion			
Key results	18	Summarise key results with reference to study objectives	10-13
Limitations	19	Discuss limitations of the study, taking into account sources of potential bias or imprecision. Discuss both direction and magnitude of any potential bias	13
Interpretation	20	Give a cautious overall interpretation of results considering objectives, limitations, multiplicity of analyses, results from similar studies, and other relevant evidence	10-13
Generalisability	21	Discuss the generalisability (external validity) of the study results	10-13
Other information			
Funding	22	Give the source of funding and the role of the funders for the present study and, if applicable, for the original study on which the present article is based	3

*Give information separately for cases and controls in case-control studies and, if applicable, for exposed and unexposed groups in cohort and cross-sectional studies.

Note: An Explanation and Elaboration article discusses each checklist item and gives methodological background and published examples of transparent reporting. The STROBE checklist is best used in conjunction with this article (freely available on the Web sites of PLoS Medicine at http://www.plosmedicine.org/, Annals of Internal Medicine at http://www.annals.org/, and Epidemiology at http://www.epidem.com/). Information on the STROBE Initiative is available at www.strobe-statement.org.

BMJ Open

Can microstructural MRI detect subclinical tissue injury in subjects with asymptomatic cervical spinal cord compression? A prospective cohort study

Journal:	*BMJ Open*
Manuscript ID	bmjopen-2017-019809.R1
Article Type:	Research
Date Submitted by the Author:	04-Jan-2018
Complete List of Authors:	Martin, Allan; University of Toronto, Department of Surgery De Leener, Benjamin; École Polytechnique de Montréal Cohen-Adad, Julien ; Polytechnique Montreal Cadotte, David; University of Calgary, Department of Neurosurgery Nouri, Aria; University of Toronto, Department of Surgery Wilson, Jefferson; University of Toronto, Department of Surgery Tetreault, Lindsay; University of Toronto, Department of Surgery; University College Cork, Department of Medicine Crawley, Adrian; University of Toronto, Department of Medical Imaging Mikulis, David; University of Toronto, Department of Medical Imaging Ginsberg, Howard; University of Toronto, Department of Medical Imaging Fehlings, Michael
Primary Subject Heading:	Neurology
Secondary Subject Heading:	Radiology and imaging, Diagnostics
Keywords:	quantitative MRI, diffusion tensor imaging, magnetization transfer, myelopathy, spinal cord injury, preclinical

Can microstructural MRI detect subclinical tissue injury in subjects with asymptomatic cervical spinal cord compression? A prospective cohort study

Allan R. Martin, MD, PhD[1],
Benjamin De Leener, PhD[2], Julien Cohen-Adad, PhD[2],
David W. Cadotte, MD, PhD[3], Aria Nouri, MD, MSc[1], Jefferson R. Wilson, MD, PhD[1],
Lindsay Tetreault, PhD[1,4], Adrian Crawley, PhD[5], David J. Mikulis, MD, PhD[5],
Howard Ginsberg, MD, PhD[5], Michael G. Fehlings, MD, PhD[5]

[1]Division of Neurosurgery, Department of Surgery, University of Toronto, Toronto, ON, Canada,
[2]Electrical Engineering, École Polytechnique de Montréal, Montréal, QC, Canada,
[3]Department of Neurosurgery, University of Calgary, Calgary, AB, Canada,
[4]Department of Medicine, University College Cork, Cork, Ireland,
[5]Department of Medical Imaging, University of Toronto, Toronto, ON, Canada

[#]Address correspondence and reprint requests to Michael G Fehlings, MD, PhD, FRCSC, FACS. Division of Neurosurgery, Toronto Western Hospital, 399 Bathurst St. Suite 4WW-449, Toronto, Ontario, M5T 2S8, Canada; Fax: 416-603-5298, Tel: 416-603-5072, E-mail: michael.fehlings@uhn.on.ca

Data Statement:
Extra data can be accessed via the Dryad data repository at http://datadryad.org/ with the doi:10.5061/dryad.kk653rs

Running title: MRI detects subclinical spinal cord tissue injury

Word Count: 3784

Abstract

Objectives: Degenerative cervical myelopathy (DCM) involves extrinsic spinal cord compression causing tissue injury and neurological dysfunction. Asymptomatic spinal cord compression (ASCC) is more common but its significance is poorly defined. This study investigates if: 1) ASCC can be automatically diagnosed using spinal cord shape analysis; 2) multiparametric quantitative MRI can detect similar spinal cord tissue injury as previously observed in DCM.

Design: Prospective observational longitudinal cohort study.

Setting: Single centre, tertiary care and research institution.

Participants: 40 neurologically intact subjects (19 female, 21 male) divided into groups with and without ASCC.

Interventions: None.

Outcome Measures: Clinical assessments: modified Japanese Orthopedic Association (mJOA) score and physical examination. 3T MRI assessments: automated morphometric analysis compared with consensus ratings of spinal cord compression, and measures of tissue injury: cross-sectional area (CSA), diffusion fractional anisotropy (FA), magnetization transfer ratio (MTR), and T2*-weighted imaging white to grey matter signal intensity ratio (T2*WI WM/GM) extracted from rostral (C1-3), caudal (C6-7), and maximally compressed levels (MCL).

Results: ASCC was present in 20/40 subjects. Diagnosis with automated shape analysis showed area under the curve > 97%. Five MRI metrics showed differences suggestive of tissue injury in ASCC compared with uncompressed subjects ($p<0.05$), while a composite of all 10 measures (average of z scores) showed highly significant differences ($p=0.002$). At follow-up (median 21 months), two ASCC subjects developed DCM.

Conclusions: ASCC appears to be common and can be accurately and objectively diagnosed with automated morphometric analysis. Quantitative MRI appears to detect subclinical tissue injury in ASCC prior to the onset of neurological symptoms and signs. These findings require further validation, but offer the intriguing possibility of pre-symptomatic diagnosis and treatment of DCM and other spinal pathologies.

Registration: Not registered.

Strengths and Limitations of this Study

Strengths:

- The development of novel spinal cord shape analysis to objectively define and detect subtle spinal cord compression
- Use of cutting-edge MRI techniques that are suitable for clinical translation to detect pre-symptomatic spinal cord tissue injury
- Multiple measures of tissue injury that cross-validate each other and can be combined as a composite to increase statistical power

Limitations:

- Lack of histopathological correlation data to confirm the presence of tissue injury
- Modest sample size makes it difficult to draw conclusions about the clinical relevance of asymptomatic cord compression because the rate of progression to symptomatic myelopathy is not well defined.

Funding

This research received funding from Rick Hansen Institute, grant number RHI-2014-12, as part of the Riluzole in Spinal Cord Injury Study (RISCIS), which is also supported by AOSpine North America, AOSpine International SCI Knowledge Forum, and the North American Clinial Trials Network (NACTN) of the Christopher and Dana Reeve Foundation. This research also received support from the Dezwirek Foundation, the Sherman Clinical Research Unit, and the Gerald and Tootsie Halbert Chair in Spinal Cord Research. Dr. Martin received post-doctoral fellowship support from Canadian Institutes of Health Research, grant number 201511MFE-359116-246227.

Conflicts of Interest

The authors declare no conflicts of interest for this manuscript.

Keywords: quantitative MRI, diffusion tensor imaging, magnetization transfer, myelopathy, spinal cord injury, preclinical

Introduction

Degenerative cervical myelopathy (DCM) involves age-related degeneration of the discs, ligaments, and vertebrae leading to extrinsic spinal cord compression and neurological dysfunction.[1] The prevalence of DCM is difficult to estimate, but it has been suggested that it is probably the most common cause of spinal cord dysfunction.[1,2] However, asymptomatic spinal cord compression (ASCC) is far more frequent, with prevalence estimates ranging from 8% to 59%.[3-8] Furthermore, spinal cord compression may be underestimated using supine MRI, which misses dynamic compression that is visible with flexion/extension MRI.[9] ASCC has received little research attention, but one study found that it confers an increased risk of myelopathy development.[10]

Emerging quantitative MRI techniques offer in vivo measurement of spinal cord microstructural features and tissue injury.[11-13] Cross-sectional area (CSA) measures spinal cord compression and atrophy, the diffusion tensor imaging (DTI) metric fractional anisotropy (FA) measures axonal integrity, magnetization transfer ratio (MTR) reflects myelin quantity, and T2*-weighted imaging (T2*WI) white matter to grey matter signal intensity ratio (T2*WI WM/GM) is a novel biomarker that we recently introduced that correlates with demyelination, gliosis, calcium, and iron concentrations.[12,14,15] These measures hold potential for earlier diagnosis of various conditions, but results to date have been modest and insufficient to drive clinical adoption.[11,13]

Our group previously reported a clinically feasible multiparametric MRI protocol that measures CSA, FA, MTR, and T2*WI WM/GM across the cervical spinal cord.[14,15] In DCM patients, these metrics reveal macro- and microstructural changes at the maximally compressed level (MCL) and in the uncompressed spinal cord above and below; significant clinical correlations and group differences compared with healthy subjects were found at rostral, MCL, and caudal levels for FA and T2*WI WM/GM, while CSA and MTR showed significant results at rostral and MCL levels.[15] In the current study, we establish an objective definition of spinal cord compression and assess newly developed automated spinal cord shape analysis for diagnostic accuracy. We test the hypothesis that subjects with ASCC experience tissue injury compared with uncompressed subjects, based on the same ten MRI measures. Finally, we investigate the rate of symptomatic myelopathy development at follow-up.

Methods

Study Design and Subjects

This study involved a secondary analysis of prospectively collected data that has been previously reported,[14,15] and received institutional approval from University Health Network (UHN, Toronto, Ontario, Canada). 42 subjects were recruited between October 2014 and December 2016 by convenience sampling and provided written informed consent. All clinical data collection and physical examinations were performed by a physician member of the UHN Spine Program. Subjects were examined to rule out neurological symptoms (numbness, weakness, fine motor dysfunction, gait/balance difficulties, urinary urgency/incontinence) and signs (hyperreflexia, weakness, sensory deficits, Romberg sign, gait ataxia). Neck pain was not considered a neurological symptom. Subjects were also

required to have 18/18 on the modified Japanese Orthopedic Association score. Two subjects were excluded during screening; one showed gait ataxia and both had sensory deficits, hyperreflexia, and MRI evidence of spinal cord compression consistent with DCM. Follow-up assessments were performed by telephone, including mJOA administration. Subjects that reported any neurological symptoms underwent a complete neurological examination in person.

MRI Acquisitions

Subjects underwent T2-weighted imaging (T2WI), DTI, magetization transfer (MT), and T2*WI at 3T (GE Signa Excite HDxt) covering C1-C7, as previously described.[14] DTI, MT, and T2*WI images were acquired with 13 axial slices from C1 to C7. T2WI was performed with a FIESTA-C sequence with 0.8x0.8x0.8 mm^3 isotropic resolution. DTI used spin-echo single shot echo planar imaging (ssEPI) with 3 acquisitions averaged offline, b = 800 s/mm^2 in 25 directions, 5 images with b=0 s/mm^2, and resolution of 1.25x1.25x5 mm^3. MT used 2D spoiled gradient echo ± MT pre-pulse, with 1x1x5mm^3 voxels. T2*WI acquisition used multi-echo recombined gradient echo (MERGE) with 3 echoes at 5,10,15 ms and resolution 0.6x0.6x4 mm^3. Total imaging time was 30-35 minutes including patient positioning, slice prescription, and 2nd order localized shimming (prior to DTI).

Image Analysis

Images were inspected and excluded from analysis if image quality was poor or artifacts were present. Quantitative imaging data were analyzed using Spinal Cord Toolbox (SCT) v3.0,[16] including spinal cord segmentation, registration to the probabilistic SCT template, and extraction of metrics with partial volume correction, as previously described.[14,15] Segmentations and registered images were reviewed, and if necessary segmentations were manually edited to correct inaccuracies.

Diagnosis of spinal cord compression followed a 3-step process. First, anatomical images (T2WI and T2*WI) were independently examined by 2 raters (ARM, AN) for indentation, flattening, torsion, or circumferential compression from extrinsic tissues (disc, ligament, or bone), and the MCL was subjectively determined. Discrepancies were resolved by consensus. Effacement of the cerebrospinal fluid (CSF) was not considered compression. Second, automated shape analysis was performed on each axial section of the T2*WI spinal cord segmentation mask. 2D principle component analysis (PCA) identified the long and short axes, representing transverse and anterior-posterior (AP) directions, respectively (Figure 1). Flattening was measured with compression ratio (CR) = AP/transverse diameter.[17] Indentation was measured using solidity = the percentage of area representing spinal cord within the convex hull that subtends the spinal cord. Torsion was measured with relative rotation, which was calculated as the angle between transverse axis and horizontal, relative to adjacent slices (difference from the average rotation of above and below slices). Circumferential compression was not specifically measured with a shape metric, as it typically coincides with flattening. Receiver operating characteristic (ROC) curves were plotted to determine diagnostic accuracy of shape metrics at each intervertebral level compared with consensus ratings. 95% confidence intervals for area under the curve (AUC) were calculated using the DeLong method with 2000 stratified bootstrap replicates. Third, discrepancies between consensus ratings and shape analysis were discussed and diagnoses were revised by consensus if necessary. The mean and SD of shape parameters were calculated in uncompressed subjects for each rostrocaudal level. Analysis of variance

(ANOVA) and Levene's test assessed if these values varied across rostrocaudal levels, in which case they were reported separately, and otherwise pooled mean, SD, and diagnostic thresholds were calculated. Optimal diagnostic thresholds were then found by maximizing Youden's Index.

Tissue injury was measured with CSA of the spinal cord, and FA, MTR, and T2*WI WM/GM extracted from WM. Metrics were normalized for rostrocaudal level and averaged across rostral (C1-3), middle (C4-5 in uncompressed subjects or maximally compressed level, MCL, in ASCC subjects), and caudal (C6-7) levels. The MCL for subjects with multilevel compression was determined by consensus ratings after considering automated shape results. For MCL measurements, data from a single level was used for CSA, whereas 3 slices centered at MCL were averaged for FA, MTR, and T2*WI WM/GM. Non-CSA metrics were also extracted from the ventral columns, lateral columns, dorsal columns and GM averaged across C1-C7 to identify focal injury. Metrics were normalized for age, sex, height, weight, and cervical cord length, similar to our previous approach,[14] based on multiple linear regression with backward stepwise variable selection. However, the presence of spinal cord compression was included to measure independent effects of other variables, and age correction was performed (regardless of significance) to mitigate group differences. Ratios of MCL/rostral metrics were also calculated.[18]

Statistical Analysis

Statistical analysis was performed with R v3.3. Numerical data were summarized by mean ± standard deviation (SD). Binary variables were compared using Fisher exact tests and numerical demographic variables were compared using two-tailed Welch's T tests. 95% confidence intervals (CIs) for frequencies were calculated using the Wilson procedure with continuity correction. MRI metrics were assumed to be normally distributed in subjects without spinal cord compression, whereas these data were assumed to be non-normal in ASCC subjects based on the hypothesis that they experience varying degrees of tissue injury. Results for individual ASCC subjects were analyzed in terms of z scores (compared to the uncompressed population), whereas group differences between ASCC and uncompressed subjects were analyzed with two-tailed Wilcoxon (non-parametric) tests. The z scores of all 10 MRI metrics (using negative values for T2*WI WM/GM) were also averaged to yield a composite score, which was assumed to follow a t distribution with 10 degrees of freedom (t_{10}) in uncompressed subjects, and results for individual subjects were analyzed using t scores. A two-tailed binomial test compared the pattern of differences (increases or decreases) in ASCC vs. uncompressed subjects with the pattern previously observed in DCM vs. healthy subjects.[15] Logistic regression with backward stepwise elimination was used to develop a model for detecting tissue injury, retaining a maximum of 4 MRI metrics as independent variables. Significance was set at $p < 0.05$ without correction for multiplicity due to the exploratory nature of this study, including individual measurements of $|z| > 1.96$, $|t_{10}| > 2.23$, and $|t_9| > 2.26$.

Results

Subject Characteristics

Subject characteristics are listed in Table 1. Individuals with ASCC were older (54.9 vs. 39.4, p=0.0007) and weighed more (79.8 vs. 71.1, p=0.03) than subjects without cord compression, while other characteristics (sex, height, and neck length) did not differ.

Table 1: Subject Characteristics. Demographics and clinical measures are tabulated for subjects with and without cervical spinal cord compression. ** denotes significant differences ($p < 0.05$) between groups.

Characteristic	Uncompressed Subjects (N=20)	Compressed Subjects (N=20)	P value
Age	39.4 ± 12.8	54.9 ± 13.8	0.0007**
Sex (M:F)	10:10	11:9	1.0
Height (cm)	172.7 ± 9.4	170.5 ± 8.0	0.43
Weight (kg)	71.1 ± 10.4	79.8 ± 13.3	0.03**
Neck Length (mm)	106.3 ± 9.6	107.0 ± 9.4	0.81

Diagnosis of Spinal Cord Compression

Consensus ratings identified 19 subjects with spinal cord compression at 41 levels (flattening: 20 levels, indentation: 30 levels, torsion: 8 levels, circumferential compression: 1 level). Relative to these ratings, automated shape analysis demonstrated an average AUC=99.2% (95% CI: 97.3% to 100%) for flattening, pooled AUC=96.8% (95% CI: 94.6% to 99.1%) for indentation, and pooled AUC=99.2% (95% CI: 98.0% to 100%) for torsion (Table 2, Figure 2). After reviewing shape analysis results, 3 levels were reclassified as flattened (total: 23 levels) and 1 level as indented (total: 31 levels). Remaining discrepancies were mostly at adjacent levels, which showed a transition between normal and abnormal shape. ANOVA detected that CR differed across rostrocaudal levels in uncompressed subjects (range: 58.7% to 67.2%), whereas solidity and relative rotation were invariant, yielding pooled normative values of 96.52% ± 0.56% and 0.3 ± 1.5 degrees, respectively.

Table 2: Shape Metrics. Data for CR, solidity, and relative rotation are displayed for each intervertebral level from C2-C7. Normal data are derived from 20 subjects with no cord compression and reported as mean ± SD. Diagnostic accuracy is reported as AUC relative to consensus ratings (prior to revised diagnoses incorporating these results). AUC: area under the curve, CR: compression ratio, ROC: receiver operating characteristic function, SD: standard deviation.

Shape Parameter	Statistic	C2-3	C3-4	C4-5	C5-6	C6-7	Pooled Values
CR (%)	Normal Mean ± SD	67.2 ± 6.4	62.6 ± 5.1	59.3 ± 4.5	59.2 ± 4.2	58.7 ± 4.5	-
	Flattened Frequency	0/40	3/40	5/40	7/40	5/40	20/200
	AUC	-	1.00	0.989	1.0	0.977	0.992
	Diagnostic Threshold	-	53.1	52.0	49.9	50.5	-
	Sensitivity		100%	97.1%	100%	97.1%	-
	Specificity		100%	100%	100%	100%	-
Solidity (%)	Normal Mean ± SD	96.52 ± 0.47	96.25 ± 0.53	96.74 ± 0.59	96.64 ± 0.46	96.45 ± 0.76	96.52 ± 0.56
	Indented Frequency	0/40	6/40	11/40	9/40	4/40	30/200
	AUC	-	0.976	0.984	0.979	1.0	0.968
	Diagnostic Threshold	-	-	-	-	-	95.6
	Sensitivity	-	-	-	-	-	88.5%
	Specificity	-	-	-	-	-	96.7%
Relative Rotation (Degrees)	Normal Mean ± SD	0.0 ± 1.3	0.5 ± 1.6	0.5 ± 1.3	0.4 ± 1.4	0.3 ± 1.5	0.3 ± 1.5
	Rotated Frequency	0/40	1/40	1/40	3/40	3/40	8/200
	AUC	-	1.0	1.0	1.0	0.991	0.992
	Diagnostic Threshold	-	-	-	-	-	3.3
	Sensitivity						97.4%
	Specificity						100%

Final diagnostic ratings identified ASCC in 20/40 subjects (50%, 95% CI: 34.1-65.9%). Six additional subjects (15%) without compression had effacement of the CSF. The frequency of ASCC increased with age (Figure 3), including 15/21 (71.4%, 95% CI: 47.7-87.8%) among subjects aged ≥ 50.

Details of spinal cord compression and shape metrics for each of the 20 ASCC subjects are provided in Supplemental Table 1. Compression was primarily anterior at all compressed levels, related to disc ± osteophyte complexes, with an element of posterior compression due to ligamentum flavum hypertrophy at 9 levels. T2WI hyperintensity was not present in any subject, although 1 had a prominent central canal (1mm diameter, within normal limits).

Variation of MRI Metrics with Age and Other Characteristics

CSA varied with cervical cord length and MTR varied with height at rostral and MCL levels, independent of the effect of cord compression (Supplemental Table 2). None of the metrics varied significantly with age.

Quantitative MRI Measures of Tissue Injury

Eight of ten age-corrected MRI metrics showed the same direction of differences in ASCC vs. uncompressed subjects as previously seen in DCM vs. healthy subjects (p=0.11), including significant differences in five metrics: increased T2*WI WM/GM at all levels (rostral: p=0.03, MCL: p=0.005, caudal: p=0.01), decreased MCL FA (p=0.04), and decreased rostral MTR (p=0.046) (Table 3). In contrast, CSA measures varied in the opposite direction from DCM, including significantly higher rostral CSA in ASCC (p=0.02). Ratios of MCL:rostral MRI metrics showed trends toward decreased FA ratio (p=0.06) and CSA ratio (p=0.09) in ASCC subjects (Table 4).

Table 3: Comparison of Normalized Quantitative MRI Metrics. Normalized MRI metrics were compared between subjects with and without cord compression. A composite Z score was used as an overall measure of tissue injury. Data extracted at the MCL were converted to Z scores to normalize for rostrocaudal variations prior to comparison and then converted back to values at C4-5 for convenience of interpretation. The direction of differences (increases/decreases) in compressed vs. uncompressed subjects was compared to previous findings in DCM vs. healthy patients. Caudal CSA and MTR were not analyzed because they did not show significant results in our prior DCM study.[15] * denotes significance (p<0.05).

Region	MRI Metric	Uncompressed (N=20)	Compressed (N=20)	P Value	Direction Matches DCM
Rostral (C1-C3)	CSA	75.4 ± 4.7	81.7 ± 9.6	0.02**	N
	FA	0.731 ± 0.031	0.720 ± 0.037	0.48	Y
	MTR	53.6 ± 3.0	51.9 ± 1.8	0.046**	Y
	T2*WI WM/GM	0.838 ± 0.029	0.863 ± 0.031	0.03**	Y
Mid (MCL or C4-5)	CSA	79.2 ± 7.7	81.9 ± 12.8	0.34	N
	FA	0.670 ± 0.044	0.631 ± 0.043	0.04**	Y
	MTR	51.1 ± 3.3	49.8 ± 2.4	0.35	Y
	T2*WI WM/GM	0.842 ± 0.019	0.864 ± 0.026	0.005**	Y
Caudal (C6-C7)	FA	0.616 ± 0.046	0.595 ± 0.051	0.24	Y
	T2*WI WM/GM	0.845 ± 0.037	0.881 ± 0.050	0.01**	Y
Composite Score		0 ± 1	-0.984 ± 1.259	0.002**	Y

Table 4: Comparison of Metric Ratios. Ratios were calculated by dividing MCL metric values by rostral values. * denotes trend (p<0.10) and ** denotes significance (p<0.05).

MCL: Rostral Ratio	Uncompressed (N=20)	Compressed (N=20)	P Value
CSA	1.050 ± 0.060	1.003 ± 0.106	0.09*
FA	0.917 ± 0.054	0.878 ± 0.056	0.06*
MTR	0.954 ± 0.042	0.960 ± 0.033	0.56
T2*WI WM/GM	1.005 ± 0.029	1.001 ± 0.025	0.67

Multivariate Results

The MRI composite score showed greater differences than single metrics (p=0.002; Table 3), including abnormal results (t_{10} score < -2.23) in 6/20 compressed subjects (Figure 4). When rostral and MCL CSA measures were replaced with CSA ratio, a revised composite score showed even stronger results ($p=8x10^{-5}$), including 9/20 compressed subjects with abnormal results (t_9 score < -2.26; Figure 4). A logistic regression model retaining MCL T2*WI WM/GM (p=0.006), FA ratio (p=0.06), CSA ratio (p=0.11), and rostral MTR (p=0.34) yielded discrimination of 0.941 between compressed and uncompressed subjects ($p=2x10^{-5}$).

Tissue Injury by Anatomical Structure

Compressed subjects had decreased FA and MTR in the ventral columns (p=0.01, 0.02, respectively), while the lateral columns, dorsal columns, and grey matter did not show significant differences in these metrics (Figure 5). In contrast, T2*WI WM/GM was increased in the lateral and dorsal columns (p=0.009, 0.0004, respectively) in compressed subjects, while the ventral columns showed no difference.

Clinical Follow-up

All 20 ASCC subjects had follow-up assessments (median: 21 months, range: 3-27 months). Four subjects reported concerning new symptoms, and following physical examination two were diagnosed with DCM (10%, 95% CI: 1.8-33.1%) and referred for surgical consultation. One experienced neck pain, intermittent right hand numbness, and gait imbalance (mJOA=17), and examination showed marked gait ataxia, asymmetric hyperreflexia, and positive left Hoffman sign. The other had neck pain, left hand numbness, and mild gait instability (mJOA=16), and examination revealed symmetric hyperreflexia and mild gait ataxia. This individual sought medical attention with her family physician, but no diagnosis was made after a new MRI was reported as “normal degenerative changes”.

Discussion

Summary of Findings

This study establishes an objective definition of spinal cord compression and found a high frequency of asymptomatic spinal cord compression, increasing in frequency with age. Multiparametric quantitative MRI provided multiple lines of evidence suggesting that ASCC involves a mild degree of spinal cord tissue injury. Significant differences were found with five MRI metrics (rostral, MCL, and caudal T2*WI WM/GM, rostral MTR, and MCL FA), with T2*WI WM/GM and MTR results suggesting that demyelination is the predominant pathophysiological mechanism in these subjects.[12,13,19] The finding of decreased MCL FA confirms two previous reports,[18,20] and may be indicative of axonal injury but could alternatively be related to demyelination.[21] However, this result could also be artifactual, as DTI metrics can be biased in the compressed spinal cord by increased susceptibility artefact,[12,21] and thus it was reassuring that MRI measures also showed changes away from the compressed region. Furthermore, the study by Lindberg et al. (2016) included only five ASCC subjects, who showed functional deficits, while the Kerkovsky et al. (2012) study

included subjects with radiculopathy, which can localize within the spinal cord GM (i.e. myeloradiculopathy). In contrast, our cohort was carefully screened to ensure the absence of neurological symptoms and signs. Recently, a larger study was completed with 92 ASCC and 71 uncompressed subjects, but DTI differences between these groups were not reported.[22] Our finding that rostral CSA was significantly greater among ASCC subjects suggests that atrophy does not occur in this condition, but rather, having a larger spinal cord appears to be a predisposing factor for compression, in keeping with a prior report that investigated spinal canal occupation ratio.[7] MCL CSA was also (non-significantly) larger in uncompressed subjects, but the ratio of MCL to rostral CSA showed a trend toward being decreased in ASCC, indicating that the mild compression observed in ASCC subjects has only a minor effect on CSA, and normalization by rostral values helps to mitigate the high inter-subject variability of this measure.[7,14] Although the groups with and without cord compression differed significantly in age and weight, all MRI metrics were corrected for age and none showed significant variation with weight. In fact, MTR and FA have previously been shown to vary with age,[11,14] but these relationships became non-significant when compression was included in the analysis, confirming a recent DTI study,[22] and suggesting that earlier studies may have overestimated the effect of age.[14,23,24] Spinal cord compression was primarily anterior in all subjects, and this appeared to preferentially cause injury to the ventral columns, as measured by reduced FA and MTR. T2*WI WM/GM demonstrated conflicting results with significant changes in lateral and dorsal columns and no significant effect in the ventral columns; we suspect that this is attributable to ventral artifacts on T2*WI, including chemical shift at the CSF-cord interface and blooming artefact from prominent anterior veins, but histopathological correlation is required. The grey matter did not show significant differences for FA or MTR, which is likely a limitation of these metrics as they are better at detecting white matter pathology.[12] Follow-up clinical data showed development of clinical myelopathy in 10% of subjects, similar to a prior report,[10] indicating that ASCC is a meaningful preclinical condition.

Our results highlight the value of multiparametric MRI and multivariate analysis; the combination of multiple tissue injury measures into a composite score is analogous (although not statistically equivalent) to taking n measurements of the same underlying value, which reduces the standard error by $1/\sqrt{n}$. This is based on the assumption that the MRI measures are covariant, measuring the common entity of tissue injury. The revised composite score showed abnormal results in nine ASCC subjects, and logistic regression suggested that the majority of subjects with ASCC experience tissue injury. However, such data-driven analysis may suffer from overfitting and must be interpreted with caution. In fact, without histopathological studies, the ground truth is unknown regarding microstructural changes that occur in ASCC, and to our knowledge no cadaver studies have investigated this topic. Overall, the results support our hypothesis at a group level, suggesting that spinal cord tissue injury begins in subjects with mild compression prior to the manifestation of clinical symptoms or signs. This offers the intriguing possibility of pre-symptomatic diagnosis in this condition and others, with far-reaching potential clinical applications. However, further investigation in a larger cohort of subjects with longer term follow-up is needed to confirm the findings of this study and to better characterize the prevalence of ASCC, relationship with age, rate of symptomatic myelopathy development, and specific prognostic factors.

An Objective Definition of Spinal Cord Compression

The high frequency of ASCC in our data are similar to the range of 51.5-66.2% (for age 40-80) reported by Kovalova et al. (2016),[8] but far higher than earlier reports of 8-26%.[3-7] These

differences are primarily due to vague and subjective definitions of spinal cord compression in prior studies, which used the terms impingement, encroachment, and compression without strict criteria.[3-7] Kerkovsky et al. (2012) provided a more precise definition of spinal cord compression: a concave defect adjacent to a bulging disc or osteophyte and/or CR < 0.4;[18] however, their threshold for CR was very low, at 4.5 SDs below the mean (based on our normative data at C5-6) and did not account for normal variations of CR across levels. Furthermore, the error associated with manual CR measurement has not been characterized, and visual assessment of concavity is subjective. Kovalova et al. (2016) provided detailed descriptions of indentation, flattening, and circumferential compression, but did not establish quantitative criteria.[8] Instead, we use automated analysis to reduce bias and define spinal cord compression as deviation from normal spinal cord morphology in 3 quantitative parameters that reflect flattening, indentation, and torsion (due to lateral bulging discs). This approach identified four levels of subtle compression missed by two expert raters and achieved excellent diagnostic accuracy. 2D PCA readily detects the transverse axis of the spinal cord, allowing calculation of CR and relative rotation, while indentation is robustly calculated using convex hulls. Several additional shape parameters are also under investigation including asymmetry indices to detect lateral compression and relative CSA to detect circumferential compression, but these were not necessary in this cohort. Automatic analysis is fast and straightforward using the free open-source Spinal Cord Toolbox,[16] and the only manual step is reviewing and editing the segmentation. Our results define normative data for each shape parameter across cervical intervertebral levels, and ROC analysis identified diagnostic thresholds that were close to 2 SDs from the mean of each metric. Many of our ASCC cases showed CSF intervening between the compressive process (e.g. disc osteophyte complex) and the ventral spinal cord surface, as the spinal cord shifts posteriorly when the subject is supine. This indicates that the cord deformity is observed in the absence of visible compression, suggesting that shape analysis can detect dynamic spinal cord compression, which has previously only been possible with flexion/extension MRI.[25]

Contemplating the Definition of Myelopathy

Myelopathy is typically defined as “a disease or disorder of the spinal cord”, and our results suggest that individuals with ASCC may meet this description. In contrast, clinicians have historically favoured functional criteria: the presence of neurological symptoms and signs that localize to the spinal cord.[26] This clinical definition most likely originated due to the lack of diagnostic investigations that can accurately detect early pathological changes within the cord. It appears that symptoms and signs of myelopathy only emerge once a considerable degree of tissue injury occurs, and we suspect that homeostatic mechanisms of neuroplasticity and behavioural adaptation act to mask early changes. Technological advances have led to the emergence of *in vivo* diagnostic tools, including MRI, that have the potential to surpass clinical assessments by taking direct measurements from the spinal cord. Similar progress has been made in electrophysiology with the development of contact heat evoked potentials (CHEPs),[27] which appear to be more sensitive than motor and sensory evoked potentials for myelopathy.[18] As these tools become more sophisticated and refined, they will allow progressively earlier detection of tissue injury in this condition, in which the ground truth likely constitutes a continuum between normal and abnormal without a clear division, similar to degenerative processes in the aging brain.

Clinical Implications

The radiological findings of mild spinal cord indentation and flattening are of unknown significance and in the authors' experience these are frequently dismissed (as seen in one subject that progressed to symptomatic myelopathy). However, the results of this study suggest that ASCC involves degradation of the tissue microstructure, likely representing a preclinical state akin to the pre-diabetic diagnosis of insulin resistance. Furthermore, these patients appear to be at increased risk for progression to clinical myelopathy, consistent with a prior study found that 8% of individuals with ASCC develop symptomatic myelopathy at 1 year and 22.6% at 4 years, with risk factors including presence of radiculopathy, T2WI hyperintensity, or prolonged conduction on electrophysiology studies.[10] Thus, individuals with ASCC should be educated about myelopathy symptoms, and further research is warranted to determine a potential role for MRI screening and longitudinal clinical follow-up. Unfortunately, patients often ignore early neurological symptoms, as was evident in two excluded subjects with evidence of mild DCM, of which they were not aware. Furthermore, additional efforts are needed to educate primary care clinicians so that prompt diagnosis of DCM can be made before debilitating symptoms have developed, at which point surgical treatment rarely restores normal ambulation and hand function. Earlier diagnosis of DCM would allow earlier treatment, and surgery is associated with reduced morbidity in all severity categories including mild DCM.[28] Preliminary results suggest that serial quantitative MRI assessments may also be helpful in detecting progression of tissue injury [29], and long-term clinical and quantitative MRI monitoring of this cohort of ASCC subjects is planned. Quantitative MRI may also hold potential for earlier diagnosis of other spinal conditions, which share pathophysiological mechanisms of demyelination, axonal injury, gliosis, and atrophy.[13]

Limitations

The statistical methods used in this study (including normalization, age correction, regression) are somewhat complex and involve several assumptions that require validation (e.g. normality). Statistical correction for multiple comparisons was not performed due to the exploratory nature of this study, but should be incorporated into the design of future confirmatory studies. The sample size of 40 subjects is too small to accurately estimate prevalence and the rate of myelopathy development, and larger confirmatory studies are required. Our normalization approach for age and other subject characteristics may be inaccurate, and ideally groups would be matched for these variables (although this is difficult because ASCC is age-related and its presence was unknown at time of recruitment). Quantitative shape analysis is dependent on an accurate spinal cord segmentation, and manual editing of segmentations was necessary in most subjects. Automatic segmentation of the compressed spinal cord is challenging due to anatomical distortion and reduced contrast with surrounding tissues, and alternative approaches are under investigation. Shape analysis would be enhanced by using an optimized high-resolution T2WI acquisition, but our T2WI had only moderate resolution and frequently showed motion artifacts. The use of convenience sampling may constitute selection bias, as individuals that have concerns of spinal pathology may be more likely to volunteer for an MRI study. Follow-up physical examinations were only performed for subjects that reported new symptoms, which could constitute information bias. The presence of metallic hardware (e.g. dental) was not grounds for exclusion, and this could bias MRI results but was not factored into the analysis. Consensus ratings for the presence of compression were used as a reference but their validity was not investigated.

Conclusions

ASCC appears to be a common age-related condition that can be accurately and objectively diagnosed with automated analysis of spinal cord morphology. Furthermore, ASCC appears to involve similar macro- and microstructural changes as symptomatic DCM, and this condition may confer an increased risk of symptomatic myelopathy development. These results require further validation, but they suggest a potential role for educating and monitoring ASCC subjects for symptoms and signs of myelopathy, while offering the possibility of presymptomatic diagnosis and treatment of other spinal pathologies.

Author Contributions

All authors provided final approval of this manuscript to be published. All authors agreed to be accountable for all aspects of the work.

Allan R. Martin: Primary contributor to study conception, design, clinical examinations of subjects, MRI data collection, image analysis, statistical analysis, and manuscript writing. This study was part of Dr. Martin's PhD thesis work at University of Toronto.

Benjamin De Leener: Contributed to study design, MRI data collection, image analysis, spinal cord shape analysis, statistical analysis, and manuscript editing.

Julien Cohen-Adad: Contributed to study design, MRI data collection, image analysis, spinal cord shape analysis, statistical analysis, and manuscript editing.

David W. Cadotte: Contributed to study design, statistical analysis, and manuscript editing.

Aria Nouri: Contributed to study design, clinical examinations, MRI data collection, image analysis, statistical analysis, and manuscript editing.

Jefferson R. Wilson: Contributed to statistical analysis, and manuscript editing.

Lindsay Tetreault: Contributed to MRI data collection, statistical analysis, and manuscript editing.

Adrian Crawley: Contributed to study design, statistical analysis, and manuscript editing.

David J. Mikulis: Contributed to study design, statistical analysis, and manuscript editing.

Howard Ginsberg: Contributed to study design, statistical analysis, and manuscript editing.

Michael G. Fehlings: Senior author and PhD supervisor to Dr. Martin. Contributed to study conception, design, clinical examinations, statistical analysis, and manuscript editing.

References

1. Nouri A, Tetreault L, Singh A, Karadimas SK, Fehlings MG. Degenerative Cervical Myelopathy: Epidemiology, Genetics, and Pathogenesis. Spine (Phila Pa 1976) 2015;40:E675-93.
2. Kalsi-Ryan S, Karadimas SK, Fehlings MG. Cervical spondylotic myelopathy: the clinical phenomenon and the current pathobiology of an increasingly prevalent and devastating disorder. Neuroscientist 2013;19:409-21.
3. Teresi LM, Lufkin RB, Reicher MA, et al. Asymptomatic degenerative disk disease and spondylosis of the cervical spine: MR imaging. Radiology 1987;164:83-8.
4. Boden SD, McCowin PR, Davis DO, Dina TS, Mark AS, Wiesel S. Abnormal magnetic-resonance scans of the cervical spine in asymptomatic subjects. A prospective investigation. J Bone Joint Surg Am 1990;72:1178-84.
5. Matsumoto M, Fujimura Y, Suzuki N, et al. MRI of cervical intervertebral discs in asymptomatic subjects. J Bone Joint Surg Br 1998;80:19-24.
6. Lee MJ, Cassinelli EH, Riew KD. Prevalence of cervical spine stenosis. Anatomic study in cadavers. J Bone Joint Surg Am 2007;89:376-80.
7. Kato F, Yukawa Y, Suda K, Yamagata M, Ueta T. Normal morphology, age-related changes and abnormal findings of the cervical spine. Part II: Magnetic resonance imaging of over 1,200 asymptomatic subjects. Eur Spine J 2012;21:1499-507.
8. Kovalova I, Kerkovsky M, Kadanka Z, et al. Prevalence and Imaging Characteristics of Nonmyelopathic and Myelopathic Spondylotic Cervical Cord Compression. Spine (Phila Pa 1976) 2016;41:1908-16.
9. Bartlett RJ, Hill CA, Rigby AS, Chandrasekaran S, Narayanamurthy H. MRI of the cervical spine with neck extension: is it useful? Br J Radiol 2012;85:1044-51.
10. Bednarik J, Kadanka Z, Dusek L, et al. Presymptomatic spondylotic cervical myelopathy: an updated predictive model. Eur Spine J 2008;17:421-31.
11. Martin AR, Aleksanderek I, Cohen-Adad J, et al. Translating state-of-the-art spinal cord MRI techniques to clinical use: A systematic review of clinical studies utilizing DTI, MT, MWF, MRS, and fMRI. Neuroimage Clin 2016;10:192-238.
12. Stroman PW, Wheeler-Kingshott C, Bacon M, et al. The current state-of-the-art of spinal cord imaging: Methods. Neuroimage 2014;84:1070-81.
13. Wheeler-Kingshott CA, Stroman PW, Schwab JM, et al. The current state-of-the-art of spinal cord imaging: Applications. Neuroimage 2014;84:1082-93.
14. Martin AR, De Leener B, Cohen-Adad J, et al. Clinically feasible microstructural MRI to quantify cervical spinal cord tissue injury using DTI, MT, and T2*-weighted imaging: assessment of normative data and reliability. AJNR 2017;In press.
15. Martin AR, De Leener B, Cohen-Adad J, et al. A Novel MRI Biomarker of Spinal Cord White Matter Injury: T2*-weighted White Matter to Grey Matter Signal Intensity Ratio. AJNR 2017;In press.
16. De Leener B, Levy S, Dupont SM, et al. SCT: Spinal Cord Toolbox, an open-source software for processing spinal cord MRI data. Neuroimage 2017;145:24-43.
17. Kameyama T, Hashizume Y, Ando T, Takahashi A. Morphometry of the normal cadaveric cervical spinal cord. Spine (Phila Pa 1976) 1994;19:2077-81.
18. Kerkovsky M, Bednarik J, Dusek L, et al. Magnetic resonance diffusion tensor imaging in patients with cervical spondylotic spinal cord compression: correlations between clinical and electrophysiological findings. Spine (Phila Pa 1976) 2012;37:48-56.
19. Cohen-Adad J. What can we learn from T2* maps of the cortex? Neuroimage 2014;93 Pt 2:189-200.

20. Lindberg PG, Sanchez K, Ozcan F, et al. Correlation of force control with regional spinal DTI in patients with cervical spondylosis without signs of spinal cord injury on conventional MRI. Eur Radiol 2016;26:733-42.
21. Cohen-Adad J, El Mendili MM, Lehericy S, et al. Demyelination and degeneration in the injured human spinal cord detected with diffusion and magnetization transfer MRI. Neuroimage 2011;55:1024-33.
22. Kerkovsky M, Bednarik J, Jurova B, et al. Spinal Cord MR Diffusion Properties in Patients with Degenerative Cervical Cord Compression. J Neuroimaging 2017;27:149-57.
23. Mamata H, Jolesz FA, Maier SE. Apparent diffusion coefficient and fractional anisotropy in spinal cord: Age and cervical spondylosis-related changes. J Magn Reson Imaging 2005;22:38-43.
24. Taso M, Girard OM, Duhamel G, et al. Tract-specific and age-related variations of the spinal cord microstructure: a multi-parametric MRI study using diffusion tensor imaging (DTI) and inhomogeneous magnetization transfer (ihMT). Nmr Biomed 2016;29:817-32.
25. Nouri A, Martin AR, Mikulis DJ, Fehlings MG. Magnetic resonance imaging assessment of degenerative cervical myelopathy: A review of structural changes and measurement techniques. Neurosurgical Focus 2016;40:E5.
26. Seidenwurm DJ, Expert Panel on Neurologic I. Myelopathy. AJNR Am J Neuroradiol 2008;29:1032-4.
27. Jutzeler C, Ulrich A, Huber B, Rosner J, Kramer J, Curt A. Improved diagnosis of cervical spondylotic myelopathy with contact heat evoked potentials. J Neurotrauma 2017.
28. Fehlings MG, Wilson JR, Kopjar B, et al. Efficacy and safety of surgical decompression in patients with cervical spondylotic myelopathy: results of the AOSpine North America prospective multi-center study. J Bone Joint Surg Am 2013;95:1651-8.
29. Martin AR, De Leener B, Cohen-Adad J, et al. Toward Clinical Translation of Quantitative Spinal Cord MRI: Serial Monitoring to Identify Disease Progression in Patients with Degenerative Cervical Myelopathy. International Society for Magnetic Resonance in Medicine. Honolulu, Hawaii, USA2017.

Figure Captions

Figure 1: Automatic Shape Analysis. T2*WI of asymptomatic subjects showing flattening (A), indentation (B), and torsion (C) of the spinal cord. D: the spinal cord segmentation (red) is analyzed with 2D PCA to identify the long (transverse) and short (AP) axes (green) that intersect at the centre of mass, and CR is calculated as ratio of AP to transverse diameters to measure flattening. E: a convex hull (green) is computed that surrounds the segmentation (red), and solidity is calculated as the ratio of segmented area to subtended area. F: the angle between the transverse axis and horizontal is computed, and then relative rotation is calculated as the ratio between the current slice and average angle in slices above and below.

Figure 2: Receiver Operating Characteristic (ROC) Curves for Diagnosis of Spinal Cord Compression using Automated Morphometric Analysis. The results of automated shape analysis to diagnosis spinal cord compression were compared against consensus ratings and ROC curves were plotted. The optimal threshold (maximizing Youden's Index) is displayed, along with the sensitivity and specificity at that level. 95% confidence intervals for AUC are calculated using the Delong method.

Figure 3: Frequency of ASCC by Decade. The frequency of ASCC is plotted against decade of life, with data for each decade provided in parentheses. ASCC: asymptomatic spinal cord compression.

Figure 4: Distributions of Composite Scores. Top: histograms (bars) of composite scores (average of the z scores of 10 MRI metrics) are displayed for subjects with ASCC (red) and no cord compression (blue). The expected distribution of results based on the null hypothesis (t distribution with ten d.f.s) is superimposed. Six ASCC subjects had abnormally low composite score ($t_{10} < -2.23$) and group differences were significant (Wilcoxon test: p=0.002). Bottom: the same plot is displayed for a revised composite score that replaces rostral and MCL CSA measures with CSA ratio, and the corresponding t distribution with nine degrees of freedom. Nine ASCC subjects had abnormal scores ($t_9 < -2.26$) and stronger group differences were found (p=0.00008).

Figure 5: Quantitative MRI Metrics by Anatomical Structure. Images include a FA map (A), a MTR map (B), and a T2*-weighted image (C) of C3-4 in an uncompressed subject. Panels D-F show the SCT probabilistic maps of the VCs (yellow), LCs (blue), DCs (red), and GM (green) overlaid. DCs: dorsal columns, FA: fractional anisotropy, GM: grey matter, LCs: lateral columns, MTR: magnetization transfer ratio, SCT: Spinal Cord Toolbox, VCs: ventral columns.

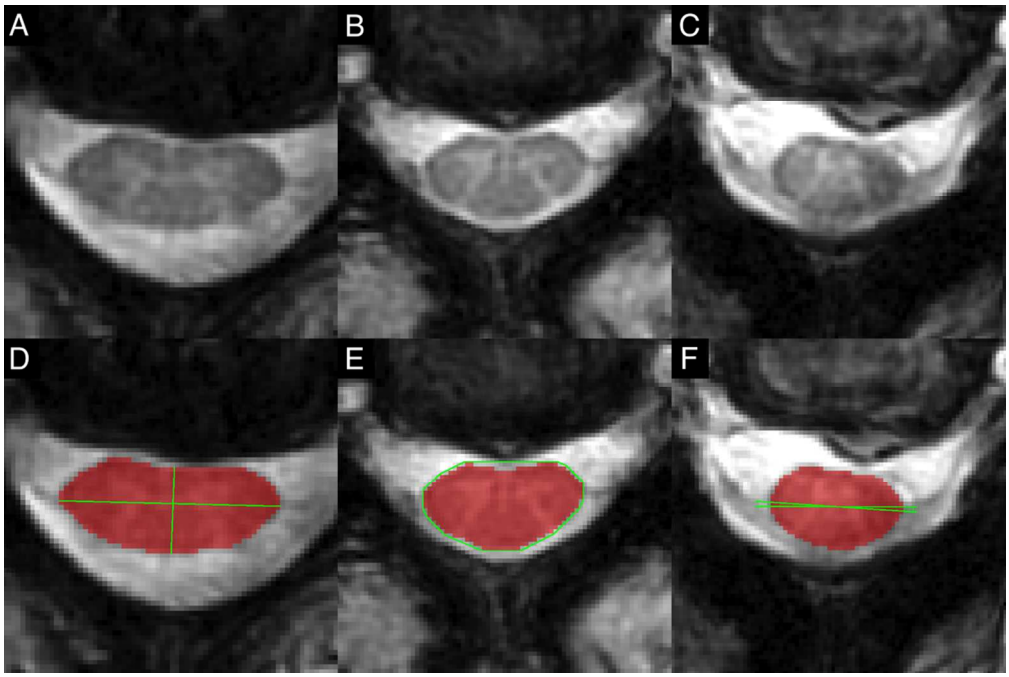

Figure 1: Automatic Shape Analysis. T2*WI of asymptomatic subjects showing flattening (A), indentation (B), and torsion (C) of the SC. D: the SC segmentation (red) is analyzed with 2D PCA to identify the long (transverse) and short (AP) axes (green) that intersect at the centre of mass, and CR is calculated as ratio of AP to transverse diameters to measure flattening. E: a convex hull (green) is computed that surrounds the segmentation (red), and solidity is calculated as the ratio of segmented area to subtended area. F: the angle between the transverse axis and horizontal is computed, and then relative rotation is calculated as the ratio between the current slice and average angle in slices above and below.

101x67mm (300 x 300 DPI)

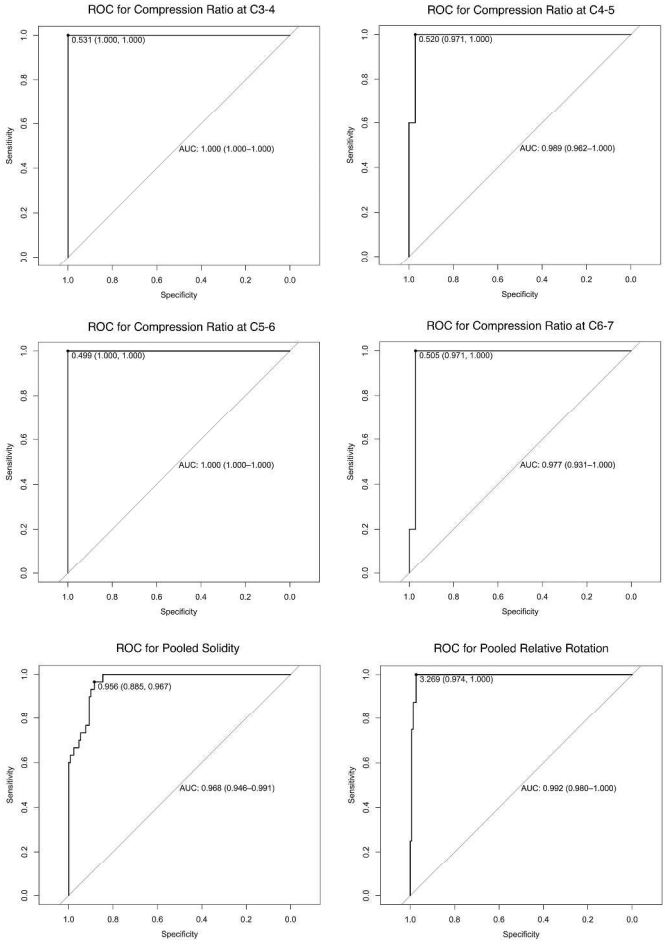

Figure 2: Receiver Operating Characteristic (ROC) Curves for Diagnosis of Spinal Cord Compression using Automated Morphometric Analysis. The results of automated shape analysis to diagnosis spinal cord compression were compared against consensus ratings and ROC curves were plotted. The optimal threshold (maximizing Youden's Index) is displayed, along with the sensitivity and specificity at that level. 95% confidence intervals for AUC are calculated using the Delong method.

156x274mm (600 x 600 DPI)

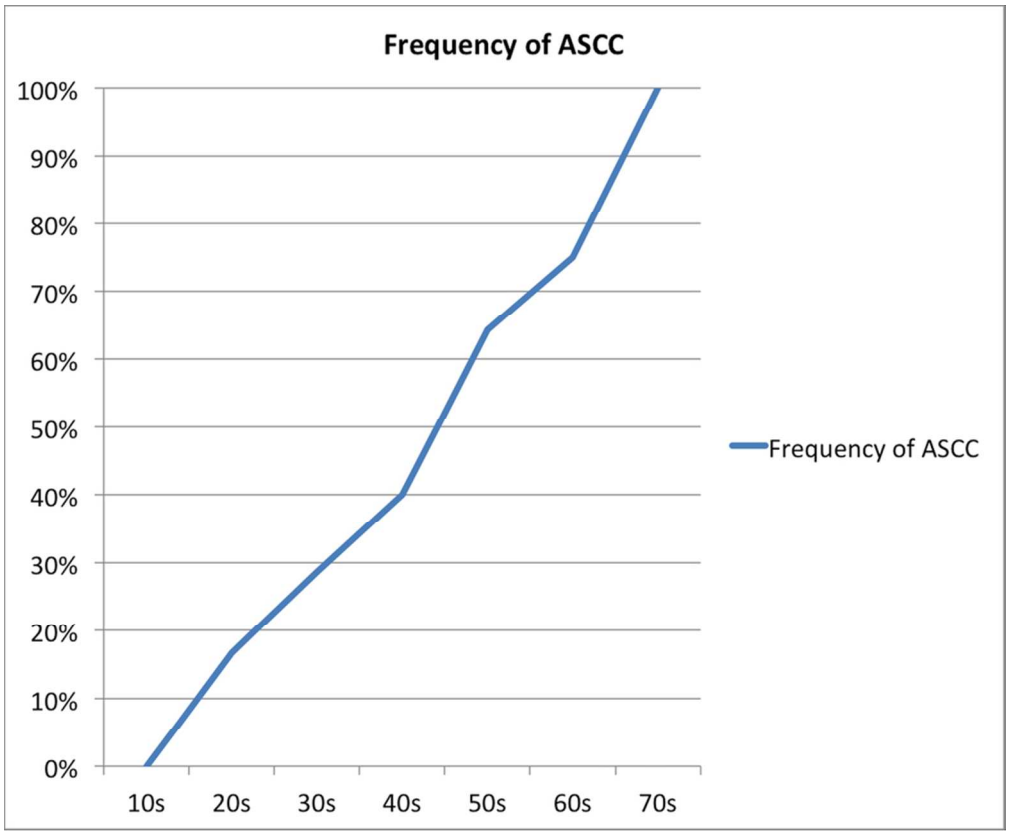

Figure 3: Frequency of ASCC by Decade. The frequency of ASCC is plotted against decade of life, with data for each decade provided in parentheses. ASCC: asymptomatic spinal cord compression.

84x69mm (300 x 300 DPI)

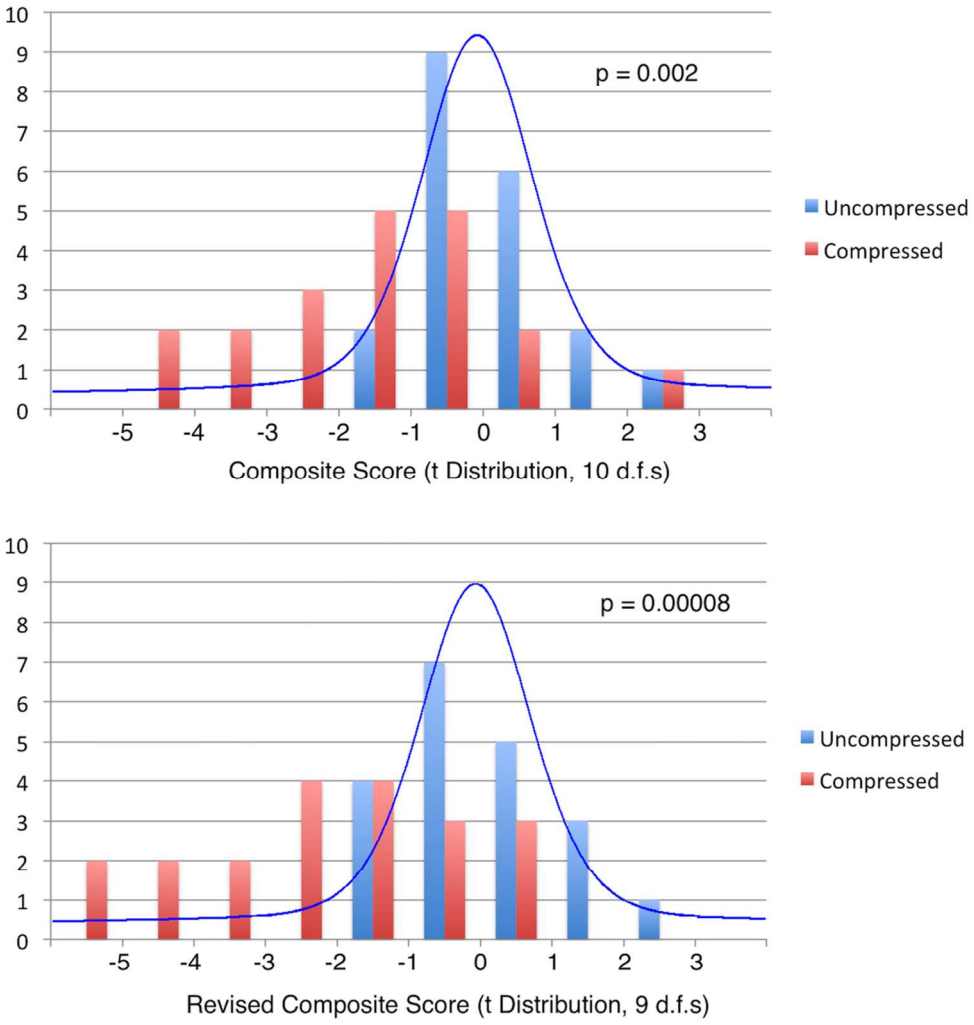

Figure 4: Distributions of Composite Scores. Top: histograms (bars) of composite scores (average of the z scores of 10 MRI metrics) are displayed for subjects with ASCC (red) and no cord compression (blue). The expected distribution of results based on the null hypothesis (t distribution with ten d.f.s) is superimposed. Six ASCC subjects had abnormally low composite score (t10 < -2.23) and group differences were significant (Wilcoxon test: p=0.002). Bottom: the same plot is displayed for a revised composite score that replaces rostral and MCL CSA measures with CSA ratio, and the corresponding t distribution with nine degrees of freedom. Nine ASCC subjects had abnormal scores (t9 < -2.26) and stronger group differences were found (p=0.00008).

111x120mm (300 x 300 DPI)

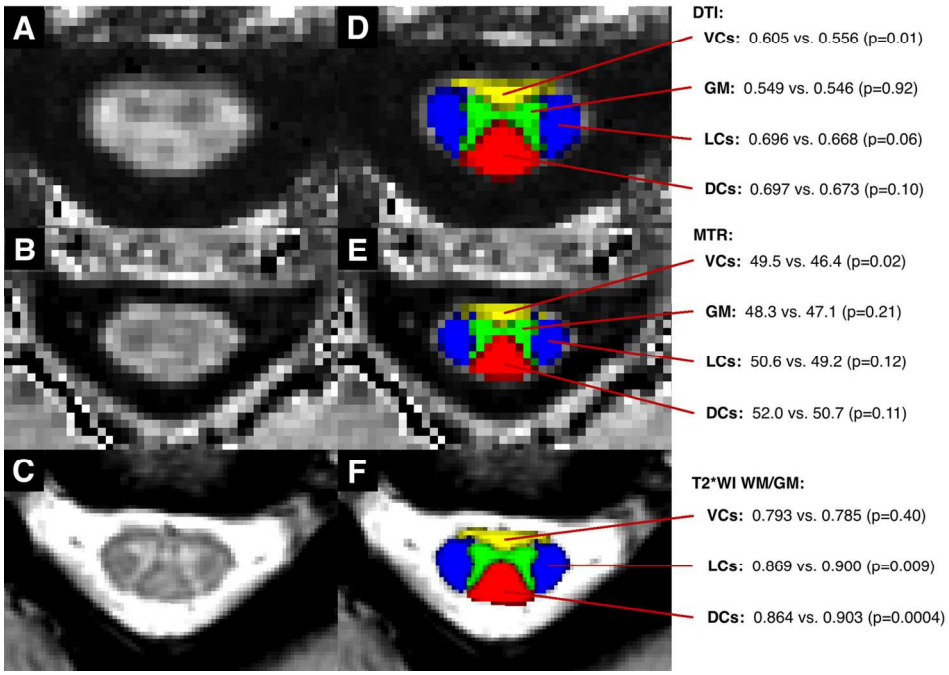

Figure 5: Quantitative MRI Metrics by Anatomical Structure. Images include a FA map (A), a MTR map (B), and a T2*-weighted image (C) of C3-4 in an uncompressed subject. Panels D-F show the SCT probabilistic maps of the VCs (yellow), LCs (blue), DCs (red), and GM (green) overlaid. DCs: dorsal columns, FA: fractional anisotropy, GM: grey matter, LCs: lateral columns, MTR: magnetization transfer ratio, SCT: Spinal Cord Toolbox, VCs: ventral columns.

139x102mm (300 x 300 DPI)

Supplemental Tables

Supplemental Table 1: Anatomical Features of Spinal Cord Compression and Quantitative Shape Metrics. MRI images were analyzed for degenerative changes causing cervical spinal cord compression, defined as indentation, flattening, or focal torsion. Levels with cord compression are listed, and a description of the degenerative changes and morphology of cord compression are provided. * denotes an abnormal value of CR, solidity, or RR. ASCC: asymptomatic spinal cord compression, CR: compression ratio, DOC: disc ± osteophyte complex, LF: ligamentum flavum, MCL: maximally compressed level, RR: relative rotation, Sol.: solidity.

#	Age, Sex	MCL	Comp. Levels	CR (%)	Sol. (%)	RR (°)	MRI Features
1	74M	C5-6	C4-5	51.5*	95.8	-1.4	Broad DOC flattening cord
			C5-6	49.3*	96.4	0.3	Broad DOC flattening cord
			C6-7	48.6*	95.2	-2.3	Lateral DOC flattening and rotating cord
2	55F	C3-4	C3-4	53.1*	93.9*	-1.0	Central DOC indenting and flattening cord, mild LF hypertrophy
			C4-5	51.7*	94.6*	-0.7	Central DOC indenting and flattening cord, mild LF hypertrophy
3	59F	C5-6	C3-4	47.8*	95.3*	1.3	Broad DOC flattening and indenting cord
			C4-5	48.5*	96.1	0.5	Broad DOC flattening cord
			C5-6	45.6*	98.2	0.5	Broad DOC flattening cord
4	28M	C4-5	C3-4	57.8	95.4*	-1.2	Central DOC indenting cord
			C4-5	53.4	94.4*	-1.0	Central DOC indenting cord
			C5-6	51.7	95.4*	-1.4	Central DOC indenting cord
5	30M	C5-6	C5-6	55.4	94.6*	2.1	Central DOC indenting cord
			C6-7	53.9	93.9*	2.1	Central DOC indenting cord
6	52F	C4-5	C3-4	56.4	94.3*	-1.8	Central DOC indenting cord, mild LF hypertrophy at C3-4, C4-5
			C4-5	60.8	92.7*	-2.9	Central DOC indenting cord, mild LF hypertrophy
			C5-6	61.1	95.4*	-7.0*	Lateral DOC indenting and rotating cord
			C6-7	48.6*	93.8*	1.0	Central DOC indenting and flattening cord
7	60F	C5-6	C5-6	50.4*	95.4*	0.7	Broad DOC flattening cord
8	69M	C5-6	C5-6	48.9*	97.5	-0.7	Broad DOC flattening cord
			C6-7	49.0*	95.8	2.5	Broad DOC flattening cord
9	66F	C4-5	C4-5	55.4	94.2*	0.0	Central DOC indenting cord, mild LF hypertrophy
10	51M	C6-7	C6-7	43.4*	91.6*	-0.9	Central DOC indenting and flattening cord
11	39M	C6-7	C6-7	55.4	94.7*	4.5*	Lateral DOC indenting and rotating cord
12	49M	C6-7	C4-5	55.2	93.7*	-0.2	Central DOC indenting cord
			C5-6	49.5*	95.8	2.1	Broad DOC flattening cord
			C6-7	46.1*	92.9*	-5.0*	Lateral DOC indenting, flattening, and rotating cord
13	50F	C5-6	C4-5	55.5	94.1*	0.5	Central DOC indenting cord
			C5-6	55.0	95.3*	-4.2*	Broad lateral DOC indenting and rotating cord
14	51F	C4-5	C3-4	55.8	95.4*	-0.8	Central DOC indenting cord
			C4-5	54.0	93.0*	1.9	Central DOC indenting cord
			C5-6	54.3	95.6	0.6	Central DOC indenting cord
15	55F	C4-5	C3-4	46.9*	96.2	0.8	Broad DOC flattening cord
			C4-5	41.3*	95.4*	0.6	Central DOC indenting cord
			C5-6	42.0*	96.0	-0.4	Broad DOC flattening cord
16	79F	C5-6	C4-5	52.3	95.5*	-1.3	Central DOC indenting cord
			C5-6	46.7*	93.3*	-2.0	Central DOC indenting and flattening cord
17	77M	C5-6	C3-4	53.2*	92.8*	-4.0*	Lateral DOC indenting and rotating cord
			C4-5	48.6*	95.8	-0.4	Broad central DOC flattening cord

			C5-6	48.3*	93.9*	-2.9*	Broad DOC indenting, flattening, and rotating cord
18	44M	C5-6	C3-4	55.6	94.9*	-0.7	Central DOC indenting cord
			C4-5	55.7	95.1*	1.4	Central DOC indenting cord
			C5-6	45.4*	93.4*	0.0	Central DOC indenting and flattening cord, mild LF hypertrophy
19	56M	C5-6	C5-6	53.6	94.8*	-1.3	Circumferential compression, flattening from broad DOC and LF hypertrophy
20	54M	C6-7	C4-5	51.5	95.3*	0.1	Central DOC indenting cord
			C6-7	46.6*	96.7	-2.4*	Broad DOC flattening and rotating cord

Supplemental Table 2: Variations of MRI Measures with Subject Characteristics. The relationship between MRI metrics and subject characteristics (age, sex, height, weight, and cervical cord length) were analyzed with backward stepwise multiple linear regression that also included a binary independent variable for the presence of cord compression. Age was retained in each model regardless of significance, and linear coefficients for age and any other significant relationships (CSA with cervical cord length and MTR with height) were subsequently used to normalize MRI metrics.

Region	MRI Metric	Age	Sex	Height	Weight	Cervical Cord Length
Rostral (C1-C3)	CSA	β=-0.168 (p=0.10)	-	-	-	β=4.81 (p=0.002)
	FA	$\beta=-6.06\times10^{-4}$ (p=0.19)	-	-	-	-
	MTR	β=-0.0472 (p=0.13)	-	β=-0.181 (p=0.0004)	-	-
	T2*WI WM/GM	$\beta=2.34\times10^{-4}$ (p=0.53)	-	-	-	-
MCL or C4-5	CSA	β=-0.195 (p=0.17)	-	-	-	β=4.90 (p=0.02)
	FA	$\beta=-7.16\times10^{-4}$ (p=0.22)	-	-	-	-
	MTR	β=-0.0545 (p=0.15)	-	β=-0.146 (p=0.01)	-	-
	T2*WI WM/GM	$\beta=3.39\times10^{-5}$ (p=0.91)	-	-	-	-
Caudal (C6-C7)	FA	β=-0.00127 (p=0.12)	-	-	-	-
	T2*WI WM/GM	$\beta=1.20\times10^{-4}$ (p=0.83)	-	-	-	-

STROBE Statement—checklist of items that should be included in reports of observational studies

	Item No	Recommendation	Page
Title and abstract	1	(*a*) Indicate the study's design with a commonly used term in the title or the abstract	2
		(*b*) Provide in the abstract an informative and balanced summary of what was done and what was found	2
Introduction			
Background/rationale	2	Explain the scientific background and rationale for the investigation being reported	4
Objectives	3	State specific objectives, including any prespecified hypotheses	4
Methods			
Study design	4	Present key elements of study design early in the paper	4-5
Setting	5	Describe the setting, locations, and relevant dates, including periods of recruitment, exposure, follow-up, and data collection	4-5
Participants	6	(*a*) *Cohort study*—Give the eligibility criteria, and the sources and methods of selection of participants. Describe methods of follow-up *Case-control study*—Give the eligibility criteria, and the sources and methods of case ascertainment and control selection. Give the rationale for the choice of cases and controls *Cross-sectional study*—Give the eligibility criteria, and the sources and methods of selection of participants	4-5 N/A N/A
		(*b*) *Cohort study*—For matched studies, give matching criteria and number of exposed and unexposed *Case-control study*—For matched studies, give matching criteria and the number of controls per case	N/A N/A
Variables	7	Clearly define all outcomes, exposures, predictors, potential confounders, and effect modifiers. Give diagnostic criteria, if applicable	5-6
Data sources/ measurement	8*	For each variable of interest, give sources of data and details of methods of assessment (measurement). Describe comparability of assessment methods if there is more than one group	4-6
Bias	9	Describe any efforts to address potential sources of bias	12
Study size	10	Explain how the study size was arrived at	13
Quantitative variables	11	Explain how quantitative variables were handled in the analyses. If applicable, describe which groupings were chosen and why	5-6
Statistical methods	12	(*a*) Describe all statistical methods, including those used to control for confounding	6
		(*b*) Describe any methods used to examine subgroups and interactions	6
		(*c*) Explain how missing data were addressed	4
		(*d*) *Cohort study*—If applicable, explain how loss to follow-up was addressed *Case-control study*—If applicable, explain how matching of cases and controls was addressed *Cross-sectional study*—If applicable, describe analytical methods taking account of sampling strategy	N/A N/A N/A
		(*e*) Describe any sensitivity analyses	N/A

Continued on next page

			Page
Results			
Participants	13*	(a) Report numbers of individuals at each stage of study—eg numbers potentially eligible, examined for eligibility, confirmed eligible, included in the study, completing follow-up, and analysed	7-10
		(b) Give reasons for non-participation at each stage	7-10
		(c) Consider use of a flow diagram	N/A
Descriptive data	14*	(a) Give characteristics of study participants (eg demographic, clinical, social) and information on exposures and potential confounders	7
		(b) Indicate number of participants with missing data for each variable of interest	N/A
		(c) *Cohort study*—Summarise follow-up time (eg, average and total amount)	7-10
Outcome data	15*	*Cohort study*—Report numbers of outcome events or summary measures over time	7-10
		Case-control study—Report numbers in each exposure category, or summary measures of exposure	N/A
		Cross-sectional study—Report numbers of outcome events or summary measures	N/A
Main results	16	(*a*) Give unadjusted estimates and, if applicable, confounder-adjusted estimates and their precision (eg, 95% confidence interval). Make clear which confounders were adjusted for and why they were included	7-10
		(*b*) Report category boundaries when continuous variables were categorized	N/A
		(*c*) If relevant, consider translating estimates of relative risk into absolute risk for a meaningful time period	N/A
Other analyses	17	Report other analyses done—eg analyses of subgroups and interactions, and sensitivity analyses	N/A
Discussion			
Key results	18	Summarise key results with reference to study objectives	10-13
Limitations	19	Discuss limitations of the study, taking into account sources of potential bias or imprecision. Discuss both direction and magnitude of any potential bias	13
Interpretation	20	Give a cautious overall interpretation of results considering objectives, limitations, multiplicity of analyses, results from similar studies, and other relevant evidence	10-13
Generalisability	21	Discuss the generalisability (external validity) of the study results	10-13
Other information			
Funding	22	Give the source of funding and the role of the funders for the present study and, if applicable, for the original study on which the present article is based	3

*Give information separately for cases and controls in case-control studies and, if applicable, for exposed and unexposed groups in cohort and cross-sectional studies.

Note: An Explanation and Elaboration article discusses each checklist item and gives methodological background and published examples of transparent reporting. The STROBE checklist is best used in conjunction with this article (freely available on the Web sites of PLoS Medicine at http://www.plosmedicine.org/, Annals of Internal Medicine at http://www.annals.org/, and Epidemiology at http://www.epidem.com/). Information on the STROBE Initiative is available at www.strobe-statement.org.